Cloud-microphysical sensors intercomparison at the Puy-de-Dôme Observatory, France

GUYOT G.[1], GOURBEYRE, C.[1], FEBVRE, G.[1], SHCHERBAKOV, V.[1,4], BURNET, F.[2], DUPONT, J.C.[3], SELLEGRI, K.[1], JOURDAN, O.[1]

[1] Laboratoire de Météorologie Physique, Université Blaise Pascal, Clermont-Ferrand, France.

[2] CNRM/GAME – Météo-France/CNRS, 42 avenue Gaspard Coriolis, 31057 Toulouse, France.

[3] Institut Pierre-Simon Laplace, Université Versailles Saint Quentin, 78280 Guyancourt, France.

[4] Laboratoire de Météorologie Physique, Institut Universitaire de Technologie d'Allier, Montluçon, France.

Correspondence to: O. Jourdan (O.Jourdan@opgc.univ-bpclermont.fr)

Abstract

Clouds play an important role in the radiative budget of the earth (Boucher et al., 2013). Since the late 70s, great advances have been made in instrumental development in order to quantify the microphysical and optical properties of clouds, both for airborne and ground-based applications. However, the cloud properties derived from these different instrumentations have rarely been compared.

In the present work, we report the results of an intercomparison campaign, performed at the Puy de Dôme during May 2013, involving a unique set of cloud instruments, located at two different places: a PVM, a FSSP, a Fog Monitor and a PWD on the roof of the station and a CDP and a SPP in a wind tunnel located underneath the roof. The main objectives of this paper are to study the effects of the wind on the ground based cloud observations with a focus on the FSSP measurements, to quantify the cloud parameters discrepancies observed by the different instruments, and to find a way to normalize the measurements.

The results reveal that most instruments show a good agreement in their sizing abilities, both in term of amplitudes and variability, but some of them have large discrepancies in their capability to assess the cloud droplet number concentrations. As a result, the total liquid water content can differ by up to a factor of 5 between the probes. The use of a standardization procedure, based on integrating probes (PVM or visibilimeter) and extinction coefficient comparison, substantially enhances the instrumental agreement. During ROSEA, the normalization coefficient range was from 0.43 to 2.2. This paper highlights the necessity to have an instrument which provides a bulk measurement of cloud microphysical or optical properties during cloud ground-based campaigns. Moreover, we show that the orientation of the probes in the main wind flow is essential for an

accurate characterization of cloud microphysical properties. In particular, FSSP experiments show strong discrepancies when the wind speed is lower than 3 $m.s^{-1}$ and when the angle between the wind direction and the orientation of the instruments is greater than 30°. Moreover, an inadequate orientation of the FSSP towards the wind direction leads to an underestimation of the measured effective diameter.

1. Introduction

The cloud droplet size distribution is one of the key parameter for a quantitative microphysical description of clouds (Pruppacher and Klett, 1997). It plays an important role in the radiative characteristics of clouds and, for example, is needed to assess the anthropogenic influence on the size and number of cloud droplets (Twomey, 1974, 1977) and on the cloud lifetime (Albrecht, 1989). Moreover, the knowledge of droplet size distribution is crucial for a better understanding of the onset of precipitation (Kenneth and Ochs, 1993) and the aerosol-cloud interaction (McFarquhar et al., 2011); according to Brenguier et al. (2003), aerosol-cloud interaction studies need accurate assessment of the cloud microphysical properties such as liquid water content (LWC), concentration and effective diameter. Moreover, the representation of liquid stratiform clouds in current climate models is relatively poor, leading to large uncertainties in climate predictions (Randall et al., 2007). Radiative, dynamic and feedback processes involved in liquid clouds still need to be studied (e.g., Petters et al., 2012, Bennartz et al., 2013) and thus require accurate measurement instrumentation. In addition, in situ measurements may be directly used for model validations, or to improve and validate remote sensing, RADAR and LIDAR retrieval algorithms.

A large set of instruments have been developed since the late 70’s to obtain precise information on cloud microphysical and optical properties. Two strategies are mainly used to measure in situ properties of clouds. The first one consists in mounting instruments on the wings of an aircraft that flies within the cloud (Gayet et al., 2009; Baumgardner et al., 2011, Brenguier et al., 2013). The other one consists in instruments operated on a ground-based platform, generally on a mountain site which altitude allows sampling natural clouds (Kamphus et al. 2010). The basic measurement principle for the size detection used in most of these devices is based on a conversion of the forward scattering of light into a size bin using the Lorentz-Mie theory (Mie, 1908). However, comparisons between the various devices reveal large discrepancies (Baumgardner, 1983, Burnet and Brenguier 1999; 2002). In addition, for the same method, studies have shown that some effects could influence the measurements, e.g., Gerber et al. (1999) highlighted the inertial concentration effect and Wendisch et al. (1998) highlighted activity corrections, changing velocity acceptance ratio, wind ramming effect, Mie curve adjustment and sensitivities to droplet size and concentration . A cloud ground based experiment performed at the Junfraujoch, Switzerland, by Spiegel et al. (2012), showed potential biases in the absolute values of the parameters, especially comparing the Fog Monitor to others instruments. Burnet and Brenguier (2002) also pointed out noticeable differences in fog measurements for airborne instrumentation, where a maximum of 30% biases were found for the LWC. Then, as recommended for airborne measurements in Brenguier et al. (2013), it is still of crucial importance to perform liquid water cloud instrumental comparison with ground based experiments.

The site of the Puy de Dôme, France, provides a unique opportunity for an intercomparison study of cloud microphysical measurements. Indeed, the station is in clouds about 50 % on the time on average (annual mean). The station consists of a platform on the roof, where a ground-based instrumentation can be installed, and a wind tunnel facing the dominant western winds used to sample air masses at air speeds up to 55 $m.s^{-1}$ in order to reproduce airborne conditions. In this paper, we will focus on the cloud instrumentation intercomparison performed within the ROSEA (Réseau d'Observatoires pour la Surveillance et l'Exploration de l'Atmosphère, i.e., Network of Monitoring centers for the Study and the Supervision of the Water

Atmospheric). The first objective is to provide a status of the instrumental variability within the cloud microphysical probes available for the scientific community to this date. A second objective is to assess the effects of the orientation of the cloud microphysical probes on the cloud droplet size distributions under different wind and cloud conditions. In particular, the response of the FSSP to non-isoaxial measurements will be investigated. As this instrument was installed on a mast, which can be oriented manually; this system allowed us to highlight the effect on the FSSP size distribution of an increasing angle between instrument orientation and wind direction.

2. Instrumentation and site

2.1 Measurement Site

The cloud microphysics instrumental intercomparison was performed at the Puy-de-Dôme atmospheric measurement station (PdD, 45.46°N, 2.57°E, 1465 m altitude), central France, in the frame of the ROSEA project (Network of Monitoring centers for the Study and the Supervision of the Water Atmospheric). The station is part of the EMEP (European Monitoring and Evaluation Programme), GAW (Global Atmosphere Watch), ACTRIS (Aerosols, Clouds, and Trace gases Research InfraStructure Network) networks where atmospheric clouds, aerosols and gases are studied.

The PdD station is located on the top of an inactive volcano rising above the surrounding area where fields and forest are predominant. The main advantage of the site is the high frequency of the cloud occurrence (50% of the time on average throughout the year). Westerly and northerly winds are dominant. Meteorological parameters, including the wind speed and direction, temperature, pressure, relative humidity and radiation (global, UV and diffuse), atmospheric trace gases (O3, NOx, SO2, CO2) and particulate black carbon (BC) are monitored continuously throughout the year (for more details see Boulon et al., 2011). Long term studies have been conducted at the site, in particular for aerosol size distribution (Venzac et al., 2009), aerosol chemical composition (Bourcier et al., 2012), aerosol optical properties (Hervo et al., 2014), aerosol hygroscopic properties (Holmgren et al., 2014), cloud chemistry (Marinoni et al., 2004; Deguillaume et al., 2014) and cloud microphysics (Mertes et al., 2001).

The ROSEA intercomparison campaign took place from the 16th to the 28th of May 2013 (see Table 1 for the details). Eleven cloudy episodes were sampled, for several hours. Temperatures were always positive, thus preventing freezing to disturb the measurements. The meteorological situation was characterized by westerly winds with speeds ranging from 1 to 22 $m.s^{-1}$. The cloud microphysical properties exhibited values of droplet effective diameter ranging between 10 and 30 µm and liquid water content (LWC) values were between 0.1 and 1 $g.m^{-3}$.

2.2. Cloud instrumentation and sampling methodology

During the ROSEA campaign, a set of instruments was deployed on the Puy de Dôme station sampling platform and in the wind tunnel to provide a description of cloud droplets from a few micrometers to 50 micrometers in terms of particle size distribution, effective diameter, extinction coefficient, LWC and number concentration. The suite of instruments mounted on the roof terrace was composed of a Forward Scattering Spectrometer Probe (PMS FSSP-100), a Fog Monitor (DMT FM-100), two PVM (Particle Volume Monitor) GERBERs and a PWD (Present Weather Detector) (see photo 1.a).

The Forward Scattering Spectrometer Probe (FSSP-100) initially manufactured by Particle Measuring Systems, Inc. of Boulder, Colorado is the oldest instrument still in use for measuring cloud droplet size distribution. The FSSP counts and sizes each droplet individually from an aspirated airstream, using forward (between the angles 4° and 12°) scattered laser-light intensity (λ = 0.633 µm) and the Mie theory, to compute the droplets size (Knollenberg, 1981). The operation, the accuracy, the limitations and the corrections are detailed by Dye and Baumgardner (1984), Baumgardner et al. (1985) and Baumgardner and Spowart (1990).For water droplet clouds, the accuracy of the derived effective diameter and liquid water content was estimated as 2 µm and 30 %, respectively (Febvre et al., 2012). According to Gayet et al. (1996), errors in particle concentration can reach 20 to 30%. In the operating range used at the Puy-de-Dôme, the resulting counts were summarized into 15 size bins, each of 3 µm width, beginning from 2 µm and ending at 47 µm of the diameter. Liquid water content was calculated by integrating the droplet volumes from the measured droplet spectrum and dividing the total mass of liquid water by the sampled air volume. The theoretical air speed through the inlet was 9 m.s^{-1}. The FSSP was checked periodically to keep the inlet facing into the wind.

The total concentration *N*, liquid water content *LWC* and extinction coefficient σ are respectively computed using the following equations (Cerni, 1983):

$$N = \sum_D \frac{n(D)}{S * TAS * \Delta t} \quad (1)$$

$$LWC = \frac{\pi}{6} * 10^{-6} * \sum_D n(D) D^3 \quad (2)$$

$$\sigma = \frac{\pi}{2} * \sum_D n(D) D^2 \quad (3)$$

where *n(D)* is the concentration measured for the size class of diameter *D*, *TAS* the speed of the air in the inlet (True Air Speed) and Δt the sampling duration. *S* is the sampling surface computed as the Depth of Field (*DOF*) multiplied by the width of the laser beam. The equation of the extinction coefficient takes into account the approximation that the extinction efficiency is equal to 2 within the droplet size and laser wavelength range. These equations are also valid for the FM 100 and the CDP. The activity correction and changing velocity acceptance ratio (Wendisch, 1998) was taken into account in the calculations. The activity correction consists of a factor, lower than 1, applied to Δt in order to take into account the losses due to instrument dead time. The others effects will be discussed below.

The Fog monitor (FM-100) is a forward scattering spectrometer probe (λ = 0.658 µm) placed in his own wind tunnel with active ventilation (Eugster et al., 2006), manufactured by Droplet Measurement Technologies, Inc., Boulder, USA , designed for use during ground-based studies. This instrument measures the number size distribution of cloud particles (with a high time resolution) in the size range between 2 and 50 µm. For the ROSEA experiments, we used a resolution of 20 channels describing the size distribution. Details about the operation of this instrument are given by Droplet Measurement Technologies (2011). According to Spiegel et al. (2012), uncertainties in concentration due to particle losses, i.e. sampling losses and losses within the FM-100 can be as high as 100 %. The FM-100 was installed on the mast next to the FSSP.

The Particle Volume Monitor (PVM-100, manufactured by Gerber Scientific, Inc., Reston, Virginia) is a ground-based forward scattering laser spectrometer for particulate volume measurements (Gerber, 1984, 1991). It is designed to measure the cloud liquid water content (*LWC*), the particle surface area (*PSA*) and to derive the droplet effective radius (r_{eff}). The PVM measures the laser light (at λ = 0.780 µm) scattered in the forward direction by an ensemble of cloud droplets which crosses the probe's sampling volume of 3 cm^3 (length of 42 cm by sampling area of 7 mm^2). The light scattered in the 0.32-3.58° angle range is collected by a system of lenses and directed through two spatial filters. The first filter converts scattered light to a signal proportional to the particle volume density (or *LWC*) of droplets; the second filter produces a signal proportional to the particle surface area density (*PSA*) (Gerber et al., 1994). From the ratio of these two quantities, r_{eff} is derived. These two filters guarantee a linear relationship between scattering intensity and *LWC* or *PSA* for droplets diameter from 3 to 45 µm (Gerber, 1991). The extinction coefficient σ is directly proportional to the *PSA*. According to Gerber et al. (1994), the accuracy of *LWC* is 10% for ~~particle diameter lower than 30 µm~~

~~and increases up to 50% for particle diameter greater than 45 µm. The study from~~ Wendish et al. (2002) ~~confirms~~ ~~the~~ ~~shortcoming of the response of a PVM-100 airborne version with increasing droplet diameter, and suggests that it begins between 20 and 30 µm, up to an efficiency of 50% for particles~~ as ~~large as 50 µm.~~

The Present Weather Detector (PWD22) is a multi-variable sensor for automatic weather observing systems. The sensor combines the functions of a forward scatter visibility meter and a present weather sensor. PWD22 can measure the intensity and the amount of both liquid and solid precipitations. As the detector is equipped with a background luminance sensor, it can also measure the ambient light (Vaisala, 2004). This instrument provides the visibility or Meteorological Optical Range (MOR), which is a measure of the distance at which an object or light can be clearly discerned and from which we can deduce the extinction coefficient σ by:

$$\sigma\ [km^{-1}] = \frac{3000}{MOR\ [m]} \tag{4}$$

According to Vaisala (2004), the accuracy of MOR and σ is 10%.

These cloud probes were operated at approximately 2 meters above the platform level. The FSSP and the FM-100 were mounted on a tilting and rotating mast allowing them to be moved manually in the dominating wind direction. The proper alignment of their inlet with the flow was based on the wind direction measurements performed by a mechanical and ultrasonic anemometer placed on a separate mast fixed on the terrace of the PdD station. A commercial pump located beneath the rotating mast was used to aspirate a constant air flow through the FSSP inlet with a sampling air speed of about 9 $m.s^{-1}$. The flow through the pump was monitored with a hot wire providing a theoretical air speed of 15 $m.s^{-1}$.

These cloud probes were operated at approximately 2 meters above the platform level. The FSSP and the FM-100 were mounted on a tilting and rotating mast allowing them to be moved manually in the dominating wind direction. The proper alignment of their inlet with the flow was based on the wind direction measurements performed by a mechanical and ultrasonic anemometer placed on a separate mast fixed on the terrace of the PdD station. A commercial pump located beneath the rotating mast was used to aspirate a constant air flow through the FSSP inlet with a sampling air speed of about 9 $m.s^{-1}$. The flow through the pump was monitored with a hot wire providing a theoretical air speed of 15 $m.s^{-1}$.

In addition to the continuous measurements performed on the station instrumental platform, the Puy de Dome research station is also equipped with an open wind tunnel located on the west side of the building. The wind tunnel consists of a 2 meter length sampling section with an adjustable airflow up to 17 $m^3.s^{-1}$ corresponding to the airspeed of 55 $m.s^{-1}$. The applied air speed inside the wind tunnel was between 10 and 55 $m.s^{-1}$. For additional information about the site description, see Bain and Gayet (1983) and Wobrock et al. (2001). During the campaign a forward scattering spectrometer probe SPP-100 model and two Cloud Droplet Probes DMT-CDPs were installed in the sampling section of the wind tunnel (see photo 1.b) to characterize the cloud microphysical properties in terms of droplet size distributions and extinction coefficients. Four experiments were performed in the wind tunnel, each with the duration of nearly two hours (see Table 1).

The SPP-100 is a modified model of the FSSP-100 from DMT with 40 size classes and a revised signal-processing package (fast-response electronic components). It has been periodically installed in the wind tunnel. Brenguier et al. (2011) have shown that the SSP-100 noticeably improve the accuracy of the size distribution assessment compare to the FSSP-100 version.

The CDP (Cloud Droplet Probe) is a forward-scattering optical spectrometer (λ = 0.658 µm), manufactured by Droplet Measurement Technologies, Inc., Boulder, USA. Light scattered by a particle is collected over a range of angles from 4 to 12° in the forward direction and then split equally between the qualifier and sizer, which allow the instrument to count and size the cloud droplets. According to Lance et al. (2010), oversizing of 60% and undercounting of 50% can occur in the CDP due to coincidence. Mie resonance structure is most pronounced for a single mode laser such as used in the CDP (Lance et al., 2010), while a multi-mode laser, as is used in the standard FSSP, can potentially dampen the Mie resonances (Knollenberg et al., 1976). As a consequence, some size bins were grouped to a total of 24 size bins, instead of 30 initially, from 3 to 49 µm. The two CDPs were installed in the wind tunnel.

During the campaign, measurements were performed with 1Hz acquisition frequency instruments. Data have been averaged over ten seconds or one minute, depending on the duration of the experiment, cloud heterogeneity, possible small gap in time synchronization of the instruments and eventual high variability of the measurements. The PVM1 measurements are provided with routine protocol which averaged the data over 5 minutes, thus any comparison with this instrument has to be carrying out with 5 minutes average data. The FSSP show incoherent measurement from March 23 to 26, probably due to electronic interferences. An overview of the data availability during the campaign is shown in Table 2.

3. Results

3.1. Data analysis strategy based on a preliminary case study

The purpose of this section is to give an overview of the microphysical measurement strategy performed during the campaign with a focus on the instrument variability. During the 16th of May a large number of instruments were deployed simultaneously on the station platform and in the wind tunnel (see Table 1).

Figure 1 provides an example of the temporal evolution of the parameters measured the 16th of May. On this graph, we choose to represent only the time series of the cloud properties when the wind tunnel was actually in function, the data are averaged over 10 seconds. The wind speed outside and inside the wind tunnel is shown on Figure 1a. The outside wind speed varied from 2 to 7 m.s^{-1} while the air speed in the wind tunnel was set up to fixed values ranging from 25 to 55 m.s^{-1}. The cloud parameters displayed on Figures 1b-1d are: the effective diameter, the number concentration and the liquid water content of cloud droplets measured by the FSSP, the PVM 2 (except for the concentration) and the FM on the roof of the PdD station as well as those ones obtained from the two CDP and the SPP located in the wind tunnel. The time series of the extinction coefficient derived from these instruments and the PWD are shown on Figure 1e. The observed cloud layers were above the freezing level with temperatures almost constant around 1 °C. During the sampling period, the dominant wind was blowing westward and the instruments positioned on the mast were oriented accordingly.

We can observe that the effective diameters of the cloud droplets are reliably sized by the different probes. Indeed both the values and the variability of the effective diameter measured by the instruments are in good agreement with a correlation coefficient close to 0.9. Only two instruments make an exception, strong discrepancies are observed when comparing the effective diameter of the PVM2 to the others instruments (Figure 1). As the discrepancies of the PVM2 can only be explained by a dysfunction of the instrument, its results were not further discussed.

The temporal evolution of the number concentration exhibit systematic differences amongst the instruments although the microphysical properties variability is well captured by all the instruments (correlation coefficient close to 0.9). The number concentration measured by the FM 100 is systematically lower than the one derived from the other instruments whereas the FSSPs (SPP and FSSP-100) show the highest values. The ratio of concentration (namely the FSSP number concentration divided by the FM number concentration) derived from these two types of instruments reaches values up to 5. Regarding the CDPs installed in the wind tunnel, the concentration measurements lie between the values obtained by the FSSPs and the FM 100. The CDPs ratio of concentration values is close to 2 between them, 1.3 between the CDP 1 and the FSSPs and 2.2 between the CDP 2 and the FSSPs. Accordingly the LWC and extinction coefficient values show significant discrepancies. The bias between the instruments is potentially very important (up to 5 when comparing the FSSPs concentration to the FM 100). At the same time, the data are well correlated (R^2 close to 0.9).

This example illustrates that the probes adequate sizing of cloud droplets is subject to a systematic bias when particle counting (number concentration) is involved. This can be clearly seen on figure 2 where the average Particle Size Distributions (PSD) measured by the different spectrometer probes are displayed.

The PSD show similar trends and shapes, with modes around 10 to 14 µm which explains the agreement in the effective diameter values. The computed average Mean Volume Diameter (~~DVM~~) shows similar values with a maximum deviation of 1.3 µm, which is within the instrumental errors. This confirms the good agreement observed between all the instruments in the qualitative parameters. However, the discrepancies observed for the magnitude (concentration) of the PSD are significant and linked to the systematic concentration bias evidenced in figure 1. This means that the size bins partitioning is correct and the number concentration discrepancies are likely to come from an incorrect assessment of the probe sampling volume. In addition, the SPP presents an overestimation of the concentration for the largest particles (larger than 30 µm), compared to the other instruments, especially for the two CDPs of the wind tunnel. One possible explanation could be the effect of ~~slashing~~ artifacts inside the SPP inlet, as evidenced by Rogers et al. (2006). This result highlights the difficulties to accurately derive the droplets concentration, which was expected due to the lack of simple number calibration for these instruments.

The red-framed parts of the time series displayed in figure 1 correspond to additional experiments where the orientation of the instruments on the mast was changed (the FM 100 and the FSSP). Those orientation changes lead to a strong decrease of all the microphysics parameters of the instruments installed on the mast, especially of the FSSP. The data corresponding to those orientation experiments are ~~then~~ removed for the following analysis. ~~The corresponding results~~ will be discussed in the section 3.4. On the example of May the 16th, we observe that the differences in concentrations measured with different probes seem to vary, and may be a function of wind speed and direction. As a consequence, we will in the next section compare instruments over the entire campaign when they all were orientated coaxially to the wind direction.

Concerning the wind tunnel, the experiments highlight the effect of the air speed applied to the measurements. Figure 3 shows the evolution of the 10 seconds average size distribution of the two CDPs present in the wind tunnel, during the experiment of the 16th of May.

During this day, the air speed in the wind tunnel varies between 25 and 55 $m.s^{-1}$, but the abrupt variations in air speed have no consequences on the size distributions of both CDP1 and CDP2. This result is applicable to the entire campaign. The air speed has to be taken into account in the calculation of the sample volume and the concentration, but the results show that the sampling of the cloud performed by the wind tunnel does not modify its microphysical properties.

3.2. Instrumental intercomparison for wind-isoaxial conditions

In this section, we focus on measurements performed in the wind tunnel and on the roof of station when the wind was isoaxial to the sampling probes inlets, over the whole campaign. Microphysical changes, due to the orientation of the instruments, observed in figure 1, will be investigated section 3.4. The data are averaged over 10 seconds for the wind tunnel measurements and over 1 minute for ambient conditions in order to make the measurements comparable (see section 2.3).

Figure 4 displays the scatter plots of the effective diameter for the instruments deployed on the PdD platform in the ambient conditions. There is a good agreement between the FM 100 and the FSSP as confirmed by the high linear correlation coefficient value (R^2=0.94). Additionally, the bias observed between these two instruments is within the “theoretical” measurement errors. The comparison between the PVM1 and the FSSP and FM-100 shows that the overall variability of cloud droplet effective diameter is well captured (R^2 close to 0.9). Even if the slope of the linear regression is greater than 1, the measurement points are close to the line 1:1 and the scatter is within the measurement uncertainties. Such discrepancy between the FM100 and the PVM has already been reported in Burnet and Brenguier (2002) and analyses are currently conducted to better understand such behavior. Moreover, the comparisons (not shown here) between the PVM 1 and the FM 100 extinction and LWC give a slope *a* of 2.1 with R^2=0.72 and a=2.6 with R^2=0.78 respectively. When comparing the PVM 1 and the FSSP 100 the slopes are a=0.35 with R^2=0.65 and a=0.4 with R^2=0.8 for the extinction and the LWC respectively. The rather good correlations obtained between the instruments as well as the comparable slope for the extinction and the LWC can be explained by the agreement of the effective diameter for the different instruments. The bias between these instruments results from a constant error stemming from the inaccurate assessment of the sampling volume or the number calibration coefficient.

The comparison between the number concentrations measured coaxially to the wind direction by the FSSP and the FM-100 over the whole campaign is displayed on Figure 5. The concentration measurements are slightly less correlated than the effective diameter measurements but the correlation remains acceptable (R^2=0.79). However, a significant discrepancy (slope of 0.15 which corresponds to a factor 6) between the instrument concentration measurements is clearly evidenced. This ratio of 6 is the same as the one obtained when LWC are compared (not shown), thus confirming that the sizing is coherent between the two instruments. The constant bias found for the concentration affects the extinction and the LWC in the same way.

Moreover the effect of the wind speed on the concentration measurements is color coded on figure 5. We can observe that the measurements performed under low wind speed conditions (lower than 5 $m.s^{-1}$) are more scattered compared to the ones corresponding to higher wind speed. We will discuss this point in details, specifically concerning the FSSP data, in Section 4.

Figure 6 shows the comparison between the 5 minutes averaged extinction coefficients measured by the PVM 1 and the PWD, two instruments that do not need an active ventilation. There is a good agreement between the two instruments ($R^2 = 0.86$) and the slope is close to 1. The discrepancies between these two instruments can be attributed to the heterogeneity of the cloud properties and the instrumental errors. The points with the low extinction values show larger variations, corresponding to the cloud edge where the properties are the most heterogeneous. However, the Pearson Principal Component Analysis shows that the correlation remains significant.

Therefore, the fact that there is a systematic constant bias (slope of 6 on Fig. 5) in the intercomparison of the droplet number concentration and of the LWC measured by the different probes, could be indicative of the inaccurate assessment of the probe sampling volume directly linked to the air flow speed measurement accuracy In order to discuss this issue, the measurements performed under ambient conditions can be confronted with the measurements in a wind tunnel where the air flow is more accurately monitored.

During the campaign a forward scattering spectrometer probe SPP-100 model and two Cloud Droplet Probes were installed in the sampling section of the wind tunnel (see photo 2). Four wind tunnel experiments were performed with a varying applied wind tunnel air speed from 10 to 55 $m.s^{-1}$ (see Table 2 for details).

Figure 7a presents the results of the effective diameter (Fig 7.a) and intercomparisons for the three instruments installed in the wind tunnel. A very good agreement amongst the probes is found, with correlation coefficients R^2 always larger than 0.9. The slope of the linear regression is close to 1, meaning that the assessment of this parameter is consistent for the CDPs and the SPP-100 thus confirming the good calibration in diameter.

The concentration intercomparisons are displayed on figure 7b. The correlation coefficient are comparable to those ones found for the effective diameter ($R^2 = 0.9$). The linear regression plots show that the slope values vary between 0.42 and 0.69 for the instruments positioned in the wind tunnel. It should be noted that these slopes are independent of the air speed applied in the wind tunnel. Even though, the discrepancies are less pronounced than that ones for the instruments placed on the platform of the PdD station, a significant bias still exists (up to a factor of 2). This bias may be attributed to the assessment of the probe sampling speed/volume. In particular, it is known that the Depth Of Field (DOF) of an instrument can be significantly different from the value given by the manufacturer. This uncertainty may exceed a factor 2 (Burnet and Brenguier, 2002) and can thus explain a large part of the biases observed between the instruments in term of concentration, extinction and LWC.

In order to evaluate the consistency of the measurements performed in ambient air (on the mast) with the ones performed in a wind controlled environment, we can characterize the relative sensitivity of the concentration measurements to the wind speeds. As seen on Figure 7, all the instruments in the wind tunnel are very well correlated. Since only the slope of the linear regression differs from one instrument to another, we choose to compare the FSSP and the FM 100 with the SPP only; as these instruments are based on the same measurement principle.

Figure 8 displays the scatter plots of the number concentration measured by the instruments on the mast against the SPP observations performed during the four wind tunnel experiments (the 16th, 22th, 24th and 28th of May with the 10 seconds average measurements). The concentrations measured by the FM 100 are rather well correlated to the SPP observations even though the wind speeds are quite different for the instruments on the roof (speeds ranging from 2 to 21 $m.s^{-1}$) compared to the instruments in the wind tunnel (air speed from 10 to 55 $m.s^{-1}$). Additionally there is no clear dependence of the measurements to the wind speed. We can thus conclude that the FM 100, the SPP and the CDPs coaxial measurements do not seem to depend on the air speed values (ambient wind speed or applied in the wind tunnel). However, a factor 4 is found between the concentrations measured on the roof by the FM-100 and by the SSP in the wind tunnel (factor 3 when compared to the CDP1). These discrepancies are once again expected considering the sample volume uncertainties (including errors on the DOF and the sampling speed that can exceed 100%), instrumental errors (around 20-30% on the concentrations for most of the instruments) and the cloud inhomogeneity.

On the contrary, the 10 seconds average FSSP measurements exhibit a high variability and show no correlation with the SPP observations. Both the inter and intra experiment variability is significant meaning that a global-data correction is not possible. Additionally, due to some instrument data availability (see Table 1), the correlation plots relative to the FSSP and the FM-100 are not directly comparable. Indeed, the 24th of May experiment is not available for the FSSP but shows a large variability in concentration, which mechanically increase the correlation of the FM 100 compared to the FSSP. However, as the FM 100 was designed for ground-based measurements, it is not surprising that the FM 100 measurements are more in accordance with the others instruments of the wind tunnel than the FSSP.

The droplet diameter and concentration intercomparisons ~~underlines~~ that the uncertainties linked to the calibration~~; and the uncertainties of~~ the calculation of the sampling volume lead to systematic biases similar for the measurement of concentration, extinction and LWC. The agreement observed between the FM 100, the SPP and the CDP measurements indicates that these data could be standardized on the base of a reference instrument with a simple relation of proportionality that would be valid for the entire campaign. However, ~~a~~ particular attention should be ~~address~~ to the FSSP measurements which were shown to be sensitive to meteorological conditions. Therefore, the remainder of this study will focus on the standardization of the results, on biases correction for isoaxial measurements as well as on the study of the effect of the air speed (wind speed or suction in the wind tunnel) on the measurements.

3.3. Improvement of data processing

The difficulties to estimate the speed of cloud particles inside the inlets, which directly impacts the assessment of the sampling volume value and derived quantities such as the number concentration, combined with the fact that there is no number calibration for the instrumentation lead to the need to standardize the recorded data. The most natural way is to standardize the measurements with the instruments which are not based on single particle counting but on the measurements of an ensemble of particles (i.e. from an integrated value). Such measurements are performed by the PVM and the PWD.

Since a good agreement was found between the extinction coefficients measured by the PVM 1 and the PWD (Fig. 6), these two instruments can be used as absolute reference of the extinction of cloud particles. As the PWD was the only instrument working during the entire campaign, all recorded data are standardized according to this instrument. Hence, the data of other instruments were averaged over 1 minute according to the PWD time resolution.

Figure 9 presents the comparison between the 1 minute averaged PWD extinctions and the data obtained in the wind tunnel for all the experiments, as a function of the wind tunnel air speed. The results show good correlations ($R^2 > 0.7$), and the slope of the regression curves corresponds to the correction coefficient ~~to apply~~ to the sampling volume of the probes. The dispersion can be attributed to the spatial difference between the instruments on the roof and in the wind tunnel and the instrumental errors. A factor of 0.44 and 0.63 ~~were~~ found, respectively for the SPP and the CDP 1. As those coefficients are linked to the modification of the sampling volume and number calibration, they can be applied to the concentration, the extinction and the LWC with a simple relation of proportionality. Moreover, Figure 9 confirms that the air speed in the wind tunnel has no influence on the measured data when the sampling volume correction is taken into account. This agrees with the results obtained for the 16th of May shown in figure 3. The measurements performed with an air speed equal to 10 $m.s^{-1}$ were removed from the dataset because of the high discrepancies observed with the PWD observations ($R^2 = 0$ for the SPP and 0.4 for the CDP 1), meaning that the sampling is inadequate at this speed. For cloud measurements, we thus recommend to use the wind tunnel with an air speed higher than 10 $m.s^{-1}$.

In a similar way figure 10 presents the comparison of the PWD extinctions with the instruments placed on the mast during the campaign, as a function of the external wind speed (right panels). The FM 100 and PWD measurements are correlated, even though the FM 100 extinction is underestimated by a factor 2 compared to the PWD reference measurements. This factor is of the same order of magnitude ~~than~~ the bias found when comparing the PWD to the instruments positioned in the wind tunnel (Figure 9). On the other hand, figure 10 shows only a poor correlation between the FSSP and the PWD extinction coefficient measurements. Additionally, the wind speed seems to have an influence on the FSSP measurements. Indeed, several points, corresponding to low wind speeds, show a large overestimation of the extinction for the FSSP. Removing the data corresponding to a wind speed lower than 5 $m.s^{-1}$, leads to a better correlation ($R^2 = 0.55$) and a slope of 0.4. It should be pointed out that the results remain almost unchanged for the FM 100 when removing the same low wind speed cases. As a consequence, the FSSP seems to be very sensitive to meteorological conditions, especially the wind conditions. Again, this reveals that low wind speeds contribute heavily towards the amount of scatter ~~and~~ so some physical phenomenon seem to affect the droplet detection (see Section 4).

Table 3 presents the summary of the instrumental intercomparison during the ROSEA campaign in term of the instrumental bias (slope *a)* and the correlation coefficient R^2. In this Table, the correlation between two instruments has been computed when the data of the two instruments were available at the same time (see Table 2), during coaxial measurements toward the wind direction and during stable cloudy periods. One minute averaged data were used to compare the instruments on the roof while. Ten seconds averaged data were used to compare instruments when wind tunnel instrumentation is involved. However, due to the time resolution (see Table 1), comparison with the PWD is made at 1 minute average and with the PVM1 at 5 minutes average. The comparisons between the PVM1 and the wind tunnel instruments are not representative due to the lack of points. Comparisons with the PWD measurements, colored in orange, give the coefficient to be applied in order to normalize the data of each instrument. All the instruments, except the FSSP, show at least an acceptable correlation ($R^2 \geq 0.6$) with the PWD during the entire campaign, independently of the meteorological conditions.

We have investigated above the coherence of performed measurements using the different probes when they were sampled isoaxially to the main wind stream. In the following, we will investigate the effect of non-isoaxial sampling on the measurements.

3.4 Effect of wind direction

In this section we focus on experiments where the mast was orientated in different directions with respect to the main wind stream. Each position was maintained during 5 minutes and the orientation was regularly moved back and forth to an isoaxial position to check if the cloud properties remained unchanged during the experiment. Four measurement series were carried out during May 22nd. The wind was blowing west all day long and the cloud properties were rather stable.

Figure 11 presents the temporal evolution of the FSSP and FM 100 size distributions along with the wind speed and the deviation angle between the instrument orientation and the wind direction. First, for the measurement with an angle equal to 0°, the cloud size distribution is almost unchanged throughout the experiment. The FSSP LWC and number concentration are approximately 1 g.m^{-3} and 1000 cm^{-3}, respectively. Then, notable changes are observed from 30° to larger angles. The concentration decreases with increasing angles and with a more pronounced impact for large water droplets (larger ~~to~~ 15 µm approximately). An impact on the small droplets is also seen for large angles, but appears to be lower for low wind speeds. Indeed, comparing the series 3 and 4 with the average values of wind speed of 7 and 3 m.s^{-1}, the size distribution shows a higher decrease in concentration when the wind is strong. The FM 100 shows the same behavior but with a lower sensitivity.

The impact of the combination of both wind speed and direction on the probe’s efficiency to sample cloud droplets is clearly illustrated on Figure 12. Figure 12 displays the cloud droplet size distribution, averaged for each angle θ and average wind speed. The percentage of the FSSP isoaxial number concentration loss for each angle and wind speed values is shown in Table 4. This percentage is computed for the total size range of droplets, for small and for large droplets, ~~arbit~~rary defined as a droplet diameter lower or greater than 14 µm respectively. On average, the greater the angular deviation from isoaxial configuration is, the more the size distribution is reduced, except for a 3 m.s^{-1} wind speed. For wind speed 5, 6 and 7 m.s^{-1}, the total percentages displayed on Table 4 go up from 74, 75 and 28 % to 95, 96 and 98%, respectively. The results also show that, for the same angle of deviation, the percentage increases with increasing wind speed, with only one exception for 30° and a wind speed of 7 $m.s^{-1}$. Thus, with increasing wind speed, the total percentage goes up from 88 to 93% for 60° and from 95 to 98% for 90°.

However for a wind speed of approximately 3 $m.s^{-1}$, the size distribution shows very small changes. Despite a ratio of about 4 between the coaxial and a deviation angle of 60°, the size distribution displays the same shape whatever the angle is. Indeed, the particle loss percentages presented on Table 4 for small and the large droplets, show very small differences compared to the other wind speed values. The size distribution could then be corrected by applying a constant factor. However, for wind speeds higher than 5 $m.s^{-1}$, the FSSP size distribution shape changes, the effective diameter decreases, if the instrument is not facing the wind. Indeed, Table 4 shows that the particle loss percentage for small particles is almost always largely lower than for larger droplets. This means that the reduction of the measured particle number due to changes in instrument orientation is more efficient for large particles. An inadequate orientation of the mast leads to an underestimation of the effective diameter. Thus, a simple correction of the size distribution is not possible if the wind is greater than 3 $m.s^{-1}$ and the deviation angle is larger than 30°.

Table 5 shows the results ~~to~~ the FM 100. For the same wind speed and direction, the values of the FM 100 concentration loss are systematically lower than the FSSP. This means that the FM 100 undergoes a weaker loss of measured particles when the instruments are not facing the wind. The variations of the FM 100 concentration loss with the wind speed and the angle are less obvious than the FSSP. Moreover, the amplitude of these variations is much weaker than the FSSP, with a minimum of 15 % and a maximum of 68 %. This confirms that the FM 100 is less sensitive to the wind speed and orientation than the FSSP-100.

4. Discussion

In order to further investigate the influence of the wind speed on the FSSP response, three additional experiments whith the SPP-100 installed on the mast along with the FSSP were performed (from the 13th to the 15th of November 2013).

The SPP has an internal estimation of the droplet speed within the sampling volume: the so-called transit speed. We recall that ideally the transit speed through the laser beam should be the same as the SPP sampling speed. In addition, this also allows us to estimate the values and the variations of the sampling volume, needed in the computation of the concentration, when assuming that the air speed is close to the particle speed. The SPP was connected to the pump used with an aspiration speed was 15 m.s^{-1} which corresponds to a theoretical sampling speed in the instrument's inlet of 9 m.s^{-1}. The instruments on the mast were always performed as coaxial measurements. The goal of this study was to use the SPP transit speed measurements to quantify the FSSP sampling volume as a function of the wind speed and the pump aspiration speed, in order to have a better understanding of the sampling processes in the inlets.

Over the period of November 13th to 15th, the wind speeds ranged from 0 to 15 m.s^{-1} and LWC values varied between 0 and 1 g.m^{-3}. The SPP transit time showed relatively high variations between 7 and 12 µs. Transit time is theoretically inversely proportional to transit speed. These values correspond to SPP transit speeds between 15 and 25 m.s^{-1}, which are higher than the theoretical value of 9 m.s^{-1} that was taken into account for the data processing of both the SPP and the FSSP. Even if the transit speed depends on the particle size distribution, these differences could explain the overestimation of the concentration and the LWC obtained from the FSSP data. It ~~underlines~~ the need of an accurate estimation of the sampling volume. Indeed, an error on the determination of the DOF or the air speed, combined with the absence of the number calibration coefficient, lead to potentially high biases even if the instruments are still capable to capture the cloud properties variations.

In order to explain the variations of the SPP transit time, it can be compared to the wind speed and the pumping speed. Figure 13 presents the comparisons of one minute averaged data. The effective diameter measured by the SPP is also shown on the colorbar. It should be pointed out that the effective diameter values higher than 20 µm were observed only during a relatively small period of time when the wind speed was below 7 $m.s^{-1}$. The transit time fluctuates independently of the wind speed or of the pump aspiration. As a consequence, there is no simple explanation to describe the absolute values and the variations of the SPP transit time.

Choularton et al. (1986) compared the FSSP volume sampling rate *V* to wind speed values. In that experiment, the ground-based FSSP was coupled with a fan with a sampling speed of 26 $m.s^{-1}$, which corresponds to a value of $V = 8{,}14\ cm^3.s^{-1}$ in windless air conditions. The wind speed varied approximately between 10 and 20 $m.s^{-1}$. The measured FSSP volume sampling rate *V* increased from 12 to 16 $cm^3.s^{-1}$ with increasing wind speed. Such values correspond to the sampling speed from 38 to 51 $m.s^{-1}$. Choularton et al. (1986) concluded that the ventilation speed and hence the volume sampling rate is modified by the ramming of air through the sample tube by the wind.

This ramming effect was not observed during our November 2013 experiments. First, the sampling air speed within the FSSP inlet was higher than expected (≥ 15 instead of 9 $m.s^{-1}$). This difference can be attributed to the underestimation of the diameter value of the instrument's laser beam (that value was set at manufacture). The results of Figure 13 show that the ramming effect cannot explain the overestimation of the concentration of the FSSP and SPP or the relatively high variability of the SPP transit time. At the same time, the variability observed in the SPP transit time measurements explains the results shown on figures 6 and 9. Indeed, in the assumption that the SPP and the FSSP have the same behavior in ground based conditions, the high variability in the FSSP sampling speed leads to high uncertainties in computed number concentrations and extinctions. That is why the FSSP number concentration and extinction show high discrepancies with the SPP and the CDP 1 (both installed in the wind tunnel) and the PWD (mounted on the roof terrace) measurements.

In addition, the variability seems to be a function of the droplet diameter. Indeed, for a diameter lower than 20 µm, the SPP transit speed varies approximately between 12 and 27 $m.s^{-1}$ whereas, for a diameter greater than 20µm, the SPP transit speed is between 15 and 20 $m.s^{-1}$. In the non-isokinetic conditions and for high Reynolds number (about $2 \cdot 10^4$), turbulent flows are expected inside and near the FSSP inlet. This could lead to strong changes in the droplets trajectories and speeds. The smaller the particle is, the more it follows the air flows. This can explain that the smallest droplets show the highest variability in the SPP transit speed. This result highlights the complex influence ~~of the~~ air flow and ~~the~~ droplet inertia may play ~~an important role~~ in the measurements.

Moreover, Gerber et al. (1999) compared the LWC measurements of the FSSP and the PVM during ground-based experiments. That study highlights the need of the knowledge of the ambient wind speed and the instrument orientation with respect to the wind direction, and suggests that the FSSP overestimates the concentration due to the droplet trajectories inside the flow accelerator when the ambient air speed is inferior to the velocity near the position of the laser. A simple trajectory model was used to understand if the suction used to draw droplets into the sampling tube of the FSSP can cause changes in the droplet concentration at the point where the laser beam interacts with the droplets. The modeling was performed for a sampling velocity of 25 m.s^{-1} and two wind-speed values of 0 and 2 m.s^{-1}. As ~~it is~~ expected, the air flow converges and accelerates into the inlet. At the same time, droplets are unable to follow the curved streamlines and, due to the droplets' inertia, show a tendency to accumulate near the centerline of the insert where the sampling volume is located. The overestimation can be determined by the enhancement factor F ~~corresponding to the ratio between FSSP measurements and the referent filter LWC of the PVM.~~ The enhancement factor decreases with increasing wind speed (from 0 to 2 m.s^{-1}) and increases with increasing droplet effective radius (from 0 to 25 µm). For a droplet radius of 25 µm, the concentration enhancement varies between a factor of 3.5 and 30 depending on the ambient air velocity. For droplet smaller than R_{eff} = 5 µm the enhancement is less than 10%. FSSP is behaving as an inertial droplet concentrator that generates spurious droplet concentration much larger than ambient values. Errors are small for droplet radius less than 5 µm but increases rapidly with increasing droplet size.

To compare our results with Gerber et al. (1999) findings, Figure 14 displays the ratio between the FSSP and PWD extinctions as a function of the effective radius provided by the FSSP and the wind speed, for the entire ROSEA campaign. The lowest values of the PWD extinction were removed in order to avoid ~~absurd~~ ratio values. The ratio of extinction or LWC (used in Gerber et al. (1999)) is the same within the hypothesis that it is due to an inaccurate assessment of the sampling volume. As we selected the PWD as the reference instrument, this ratio is similar to the enhancement factor F from Gerber et al. (1999). Our results show high values and variability of the ratio for low values of the wind speed whereas the ratio is constant (~2.5 which join the slope of 0.4 seen in the figure 10) when the wind speed is greater than 5-6 m.s^{-1}. However, it seems that there is some increase of the ratio with the droplet diameter for diameter values greater than 6 µm, which is in agreement with the conclusion of Gerber et al. (1999). For diameter lower than 6 µm, an important scatter is observed that should confirm the idea that potential turbulent flow in the inlet can sweep the smallest particles and so can alter the measurements.

Thus, a relative good agreement between the inertial concentration effect showed by Gerber et al. (1999) and our results is observed. As a consequence, we have indications which tend to show that the FSSP measurements with a wind speed too low have to be removed if any incoherence is found.

5. Conclusion

Accurate measurements of cloud microphysics properties are crucial for a better understanding of cloud processes and its impact on the climate. A large set of various cloud instrumentation were developed since the 80's. However, accurate comparisons between instruments are still scarce, in particular comparisons between ground-based and airborne conditions. To address this problem, we analyzed the results of both ground-based and wind tunnel measurements performed with various instrumentations during the ROSEA campaign at the station of the Puy-de-Dôme (Central France, 1465 m altitude) in May 2013. This instrumental intercomparison includes a FSSP, a Fog Monitor 100, a PWD, a PVM ~~on~~ ground-based conditions and two CDPs and a SPP-100 in the wind tunnel.

Our results show very good correlations between the measurements performed by the different instruments, especially, for the shape of the size distribution and the effective-diameter values. Whereas effective diameter absolute values show good agreement within the 10 % average instrument uncertainty, total-concentration values can diverge by a maximum factor of 5. ~~It~~ was expected in our study since there was no preliminary calibration in particle total-number for the instruments we used. On the other hand, comparisons between ground-based and controlled wind measurements lead to original results, which show rather good correlation, but with the same problem of the concentration-values bias. We thus propose to standardize with a reliable instrument, which doesn't use a sample volume. The data were thus normalized based on the bulk extinction coefficient measurements performed by the PWD. When comparing the extinction with the PWD, the results show that the measurements do not depend on the air speed for the instruments in the wind tunnel and on the wind speed for ground based instruments. Moreover, the measurements can be standardized with a simple relation of proportionality, with a coefficient comprised between 0.43 and 2.2 during ROSEA, which is valid for the entire campaign. However this is not applicable to the ground based FSSP measurements which were shown to be very sensitive to the wind speed and direction. Indeed, these measurements are highly variable when the wind speed was lower to the theoretical air speed through the inlet. The observed FSSP extinction overestimation, compared to the PWD, ~~has~~ showed some agreements with the Gerber et al. (1999) study, which highlights the inertial concentration effects. Moreover, additional orientation experiments were performed. The FSSP and FM orientation was modified with an angle ranging from 30° to 90° angle with wind speeds from 3 to 7 $m.s^{-1}$. The results show that the induced number concentration loss is between 29 and 98 % for the FSSP and between 15 and 68 % for the FM-100. This study revealed that it is necessary to be very critical with cloud measurements when the wind speed is lower than 3 $m.s^{-1}$ and when the angle between the wind direction and the orientation of the instruments is greater than 30°.

Finally ~~to~~ ~~explain~~ the high dispersion of the ground based FSSP measurements compared to the others instruments. The transit speed of droplets in the sampling volume was investigated using the SPP measurements on the mast. The ground based SPP observations showed a strong variability in the transit speed of the cloud droplets. This variability did not depend of the variations of the pump aspiration or the wind speed. As this effect was more pronounced for small particles, the presence of turbulent flow inside the inlet could be a plausible explanation of the discrepancies of the measurements based on particle counting.

Acknowledgements. This work was performed within the framework ROSEA (Réseau d'Observatoires pour la Surveillance et l'Exploration de l'Atmosphère) and ACTRIS (Aerosols, Clouds and Trace gases Research Infra Structure Network). It was supported by the French ANR CLIMSLIP. The authors also thank the OPGC (Observatoire de Physique du Globe de Clermont) for monitoring the PdD station.

References

Albrecht, B.A.: Aerosols, cloud microphysics, and fractional cloudiness, Science, 245, 1227-1230, 1989.

Bain, M. and Gayet, J.F.: Contribution to the modeling of the ice accretion process: ice density variation with the impacted surface angle, Ann. Glaciol., 4, 19-23, 1983.

Baumgardner, D.: An analysis and comparison of five water droplet measuring instruments, J. Appl. Meteor, 22, 891-910, 1983.

Baumgardner D., Strapp W., Dye J.E.: Evaluation of the Forward Spectrometer Probe. Part II: Corrections for coincidence and dead time losses, J. Atmos. Oceanic Technol., 2, 626-632, 1985.

Baumgardner D., Spowart M.: Evaluation of Forward Spectrometer Probe. Part III: Time response and laser Inhomogeneity limitations, J. Atmos. Oceanic Technol., 7, 666-672, 1990.

Baumgardner, D., Brenguier, J., Bucholtz, A., Coe, H., DeMott, P., Garrett, T., Gayet, J., Hermann, M., Heymsfield, A., Korolev, A., Krämer, M., Petzold, A., Strapp, W., Pilewskie, P., Taylor, J., Twohy, C.,Wendisch, M., Bachalo,W., and Chuang, P.: Airborne instruments to measure atmospheric aerosol particles, clouds and radiation: A cook's tour of mature and emerging technology, Atmos. Res., 102, 10–29, doi:10.1016/j.atmosres.2011.06.021, 2011.

Bennartz, R., Shupe, M.D., Turner, D., Walden, V.P., Steffen, K., Cox, C.J., Kulie, M.S., Miller, N.B., Pettersen, C.: July 2012 Greenland melt extent enhanced by low-level liquid clouds, Nature, 496, 83-86, doi:10.1038/nature12002, 2013.

Boucher, O., Randall, D., Artaxo, P., Bretherton, C., Feingold, G., Forster, P., Kerminen, V.-M., Kondo, Y., Liao, H., Lohmann, U., Rasch, P., Satheesh, S.K., Sherwood, S., Stevens B. and Zhang, X.Y.: Clouds and Aerosols. In: Climate Change 2013: The Physical Science Basis. Contribution of Working Group I to the Fifth Assessment Report of the Intergovernmental Panel on Climate Change, Cambridge University Press, Cambridge, United Kingdom and New York, NY, USA, 2013.

Boulon, J., Sellegri, K., Hervo, M., Picard, D., Pichon, J.-M., Fréville, P., and Laj, P.: Investigation of nucleation events vertical extent: a long term study at two different altitude sites, Atmos. Chem. Phys., 11, 5625-5639, doi:10.5194/acp-11-5625-2011, 2011.

Bourcier, L., Sellegri, K., Chausse, P., Pichon, J.M., Laj, P.: Seasonal variation of water-soluble inorganic components in aerosol size-segregated at the puy de Dôme station (1,465 ma.s.l.), France, J. Atmos. Chem., 69, 47-66, doi: 10.1007/s10874-012-9229-2, 2012.

Brenguier, J.L., Pawlowska, H., Schüller, L.: Cloud microphysical and radiative properties for parameterization and satellite monitoring of the indirect effect of aerosol on climate, J. Geophys. Res., 108, 8632, doi: 10.1029/2002JD002682, 2003.

Brenguier J.-L., Burnet, F., Geoffroy, O.: Cloud optical thickness and liquid water path. Does the k coefficient vary with droplet concentration ?, Atmos. Chem. Phys., 11, 9771-9786, doi: 10.5194/acp-11-9771-2011, 2011.

Brenguier, J.-L., Bachalo, W. D., Chuang, P. Y., Esposito, B. M., Fugal, J., Garrett, T., Gayet, J.-F., Gerber, H., Heymsfield, A., Kokhanovsky, A., Korolev, A., Lawson, R. P., Rogers, D. C., Shaw, R. A., Strapp, W. and Wendisch, M.: In Situ Measurements of Cloud and Precipitation Particles, in Airborne Measurements for Environmental Research: Methods and Instruments (eds M. Wendisch and J.-L. Brenguier), Wiley-VCH Verlag GmbH & Co. KGaA, Weinheim, Germany. doi: 10.1002/9783527653218.ch5, 2013.

Burnet F., and J. L. Brenguier: Validation of droplet spectra and liquid water content measurements, Phys. Chem. Earth (B), 24, 249-254, 1999.

Burnet F., and J. L. Brenguier: Comparison between standard and modified Forward Scattering Spectrometer Probes during the Small Cumulus Microphysics Study, J. Atmos. Oceanic Technol., 19, 1516-1531, 2002.

Cerni, T.: Determination of the size and concentration of cloud drops with an FSSP, J. Climate Appl. Meteor., 22, 1346-1355, 1983.

Choularton, T.W., Consterdine, I.E., Gardiner, B.A., Gay, M.J., Hill, M.K., Latham, J., Stromberg, M.: Field studies of the optical and microphysical characteristics of clouds enveloping Great Dun Fell, Quart. J. R. Met. Soc., 112, 131-148, 1986.

Deguillaume, L., Charbouillot, T., Joly, M., Vaïtilingom, M., Parazols, M., Marinoni, A., Amato, P., Delort, A.M., Vinatier, V., Flossmann, A., Chaumerliac, N., Pichon, J.M., Houdier, S., Laj, P., Sellegri, K., Colomb, A., Brigante, M., Mailhot, G.: Classification of clouds sampled at the puy de Dôme (France) based on 10 yr of monitoring of their physicochemical properties, Atmos. Chem. Phys., 14, 1485–1506, doi:10.5194/acp-14-1485-2014, 2014.

Droplet Measurement Technologies: Fog Monitor Model FM-100 Operator Manual (DOC-0088 Revision H), published by Droplet Measurement Technologies, Inc., Boulder, USA, 2011.

Dye, J.E., Baumgardner D.: Evaluation of the Forward Scattering Spectrometer Probe. Part I: Electronic and Optical Studies, J. Atmos. Oceanic Technol., 1, 329-344, 1984.

Eugster, W., Burkard, R., Holwerda, F., Scatena, F., and Bruijnzeel, L.: Characteristics of fog and fogwater fluxes in a Puerto Rican elfin cloud forest, Agr. Forest. Meteorol., 139, 288–306, doi:10.1016/j.agrformet.2006.07.008, 2006.

Febvre G., Gayet, J.F., Shcherbakov., V., Gourbeyre, C., Jourdan, O.: Some effects of ice crystals on the FSSP measurements in mixed phase clouds, Atmos. Chem. Phys., 12, 8963–8977, doi:10.5194/acp-12-8963-2012, 2012.

Gayet, J.F., Febvre G., Larsen, H.: The reliability of the PMS FSSP in the presence of small ice crystals, J. Atmos. Oceanic Technol., 13, 1300-1310, 1996.

Gayet, J.F., Mioche, G., Dörnbrack, A., Ehrlich, A., Lampert, A., Wendisch M.: Microphysical and optical properties of Arctic mixed-phase clouds. The 9 April 2007 case study**,** Atmos. Chem. Phys., 9, 6581–6595, 2009.

Gerber, H.: Liquid water content of fogs and hazes from visible light scattering, J. Climate Appl. Meteor., 23, 1247-1252, 1984.

Gerber, H.: Direct measurement of suspended particulate volume concentration and far-infrared extinction coefficient with a laser diffraction instrument, Appl. Optics, 30, 4824-4831, 1991.

Gerber, H., Arends, B.G., and Ackerman A.S.: New microphysics sensor for aircraft use, Atmos. Res., 31, 235–252, 1994.

Gerber, H., Frick, G., Rodi, A.R.: Ground-based FSSP and PVM Measurements of Liquid Water Content, J. Atmos. Oceanic Technol., 16, 1143-1149, 1999.

Hervo, M., Sellegri, K., Pichon, J.M., Roger, J.C. and Laj, P.: Long term measurements of optical properties and their hygroscopic enhancement, Atmos. Chem. Phys. Discuss., 14, 27731–27767, doi:10.5194/acpd-14-27731-2014, 2014.

Holmgren, H., Sellegri, K., Hervo, M., Rose, C., Freney, E., Villani, P., Laj P.: Hygroscopic properties and mixing state of aerosol measured at the high altitude site Puy de Dôme (1465 m a.s.l.), France, Atmos. Chem. Phys. Discuss., 14, 6759-6802, doi:10.5194/acpd-14-6759-2014, 2014.

Kamphus, M., Ettner-Mahl, M., Klimach, T., Drewnick, F., Keller, L., Cziczo, D. J., Mertes, S., Borrmann, S., and Curtius, J.: Chemical composition of ambient aerosol, ice residues and cloud droplet residues in mixed-phase clouds: single particle analysis during the Cloud and Aerosol Characterization Experiment (CLACE 6), Atmos. Chem. Phys., 10, 8077–8095, doi:10.5194/acp-10-8077-2010, 2010.

Kenneth, V. and Ochs, H.: Warm-rain initiation: An overwiew of Microphysical Mechanisms, J. Appl. Meteorol., 32, 608-625, 1993.

Knollenberg, R.G.: Practical Applications of Low Power Lasers, SPIE, 92, 137–152, 1976.

Knollenberg, R.G.: Techniques for probing cloud microstructure, in: Clouds, their formation, optical properties and effects, Hobbs, P.V. and Deepak, A., Academic Press, New York, USA, 15-92, 1981.

Lance, S., Brock, C.A., Rogers, D. and Gordon, J. A.: Water droplet calibration of the Cloud Droplet Probe (CDP) and in-flight performance in liquid, ice and mixed-phase clouds during ARCPAC, Atmos. Meas. Tech., 3, 1683–1706, doi:10.5194/amt-3-1683-2010, 2010.

Marinoni, A., Laj, P., Sellegri, K., and Mailhot, G.: Cloud chemistry at the Puy de Dôme: variability and relationships with environmental factors, Atmos. Chem. Phys., 4, 715-728, doi:10.5194/acp-4-715-2004, 2004.

McFarquhar, G., Ghan, S.J., Verlinde, J., Korolev, A., Strapp, J.W., Schmid, B., Tomlinson, J., Wolde, M., Brooks, S., Cziczo, D., Dubey, M., Fan, J., Flynn, C., Gultepe, I., Hubbe, J., Gilles, M., Laskin, A., Lawson, P., Leaitch, W.; Liu, P., et al.: Indirect and Semi-Direct Aerosol Campaign: The Impact of Arctic Aerosols on Clouds, B. Am. Meteorol. Soc., 92, 183-201, doi:10.1175/2010BAMS2935.1, 2011.

Mertes, S., Schwarzenböck, A., Laj, P., Wobrock, W., Pichon, J.M., Orsi, G., Heintzenberg, J.: Changes of cloud microphysical properties during the transition from supercooled to mixed-phase conditions during CIME, Atmos. Res., 58, 267-294, 2001.

Mie, G.: Beiträge zur Optik trüber Medien, speziell kolloidaler Metallösungen, Ann. Phys.-Berlin, 330, 377–445, 1908.

Petters, J.L., Harrington, J.Y., Clothiaux, E.: Radiative-dynamical feedbacks in low liquid water path stratiform clouds, J. Atmos. Sci., 69, 1498–1512, DOI: 10.1175/JAS-D-11-0169.1, 2012.

Pruppacher, H. R. and Klett, J. D.: Microphysics of Clouds and Precipitation, Kluwer Academic Publishers, Dordrecht, 1997.

Randall, D. A., and Coauthors: Climate models and their evaluation. Climate Change 2007: The Physical Science Basis, S. Solomon et al., Eds., Cambridge University Press, 589–662, 2007.

Rogers, D., Stith, J., Jensen, J., Cooper, W., Nagel, D., Maixner, U. and Goyea, O.: Splash artifacts in FSSP measurements; observations and flow modeling studies, 12th conference of cloud physics, Madison, USA, 10 – 14 July 2006, P2.30, 2006.

Rose, C., Boulon, J., Hervo, M., Holmgren, H., Asmi, E., Ramonet, M., Laj, P., and Sellegri, K.: Long-term observations of cluster ion concentration, sources and sinks in clear sky conditions at the high-altitude site of the Puy de Dôme, France, Atmos. Chem. Phys., 13, 11573-11594, doi:10.5194/acp-13-11573-2013, 2013.

Spiegel, J.K., Zieger, P., Bukowiecki, N., Hammer E., Weingartner, E. and Eugster, W.: Evaluating the capabilities and uncertainties of droplet measurements for the fog droplet spectrometer (FM-100), Atmos. Meas. Tech., 5, 2237–2260, doi:10.5194/amt-5-2237-2012, 2012.

Twomey, S.: Pollution and the planetary albedo, Atmos. Environ., 8, 1251-1256, 1974.

Twomey, S.: The influence of pollution on the shortwave albedo of clouds, J. Atmos. Sci., 34, 1149–-1152, 1977.

Vaisala: Present Weather Detector PWD22 user’s guide, published by Vaisala, Helsinki, Finland, 2004.

Venzac, H., Sellegri, K., Villani, P., Picard D., Laj, P.: Seasonal variation of aerosol size distributions in the free troposphere and residual layer at the Puy de Dôme station, France, Atmos. Chem. Phys., 9, 1465-1478, doi:10.5194/acp-9-1465-2009, 2009.

Wendisch, M. : A quantitative comparison of ground-based FSSP and PVM measurements, J. Atmos. Oceanic Technol., 15, 887-900, 1998.

Wendisch, M., Garrett, T.J., Strapp, J.W.: Wind tunnel tests of airborne PVM-100A response to large droplets, J. Atmos. Oceanic Technol., 19, 1577-1584, 2002.

Wobrock, W., Flossmann, A., Monier, M., Pichon, J.M., Cortez, L., Fournol, J.F., Schwarzenböck, A., Mertes, S., Heintzenberg, J., Laj, P., Orsi, G., Ricci, L., Fuzzi, S., Brink, H.T., Jongejan, P., Otjes, R.: The Cloud Ice Mountain Experiment (CIME) 1998: experiment overview and modeling of the microphysical processes during the seeding by isentropic gas expansion, Atmos. Res., 58, 231-265, 2001.

Tables

	Wind tunnel			Roof					
Date	SPP	CDP 1	CDP 2	FSSP	PVM 1	PVM 2	PWD	FM 100	meteo
16/05/2013	√	√	√	√	×	√	√	√	cloudy
17/05/2013	×	×	×	√	√	×	√	√	cloudy
19/05/2013	×	×	×	√	√	×	√	√	cloudy
20/05/2013	×	×	×	√	√	×	√	√	cloudy
21/05/2013	×	×	×	√	×	×	√	√	cloudy
22/05/2013	√	√	×	√	×	×	√	√	cloudy
23/05/2013	×	×	×	×	~	~	√	√	cloudy
24/05/2013	√	√	×	×	×	√	√	√	cloudy
25/05/2013	×	×	×	×	√	√	√	√	cloudy
26/05/2013	×	×	×	×	√	√	√	√	cloudy
27/05/2013	×	×	×	√	√	√	√	√	clear
28/05/2013	√	√	×	√	√	√	√	√	cloudy

√ = data available

~ = data available during a part of the day

× = data not available

Table 1: Data availability for each instrument used during ROSEA

Instrument	Measured parameter(s)	Measurement range	Accuracy	Time resolution
Forward Scattering Spectrometer Probe (FSSP & SPP)	size distribution	2 - 47 µm	D : ±3µm Number conc : ±20%	1 sec
Fog Monitor (FM)	size distribution	2 - 50 µm	D : ±3µm Number conc : ±100%	1 sec
Cloud Droplet Probe (CDP)	size distribution	2 - 50 µm	D : ±3µm Number conc : ±50%	1 sec
Particle Volume Monitor (PVM)	extinction, LWC, Reff	2 - 70 µm	LWC : ±10%	PVM1 : 5 min PVM2 : 1 sec
Present Weather Detector (PWD 22)	extinction	all	±10%	1 min

Table 2: Instrumental set-up during the ROSEA intercomparision campaign at the Puy-de-Dôme

	Roof			Wind tunnel		
	FM 100	PVM1	FSSP	SPP	CDP1	CDP2
PWD	a=2,23 ; R^2=0,58	a=1,17 ; R^2=0,86	a=0,35 ; R^2=0,24	a=0,44 ; R^2=0,86	a=0,63 ; R^2=0,72	a=1,05 ; R^2=0,72
FM 100		a=0,45 ; R^2=0,74	a=0,15 ; R^2=0,79	a=0,26 ; R^2=0,61	a=0,39 ; R^2=0,61	a=0,46 : R^2=0,61
PVM1			a=0,34 ; R^2=0,64	/	/	/
FSSP				no correlation	no correlation	no correlation
SPP					a=0,69 ; R^2=0,95	a=0,42 ; R^2=0,91
CDP1						a=0,59 ; R^2=0,91
CDP2						

Table 3: Summary of the cloud extinction coefficient intercomparison performed during ROSEA. The coefficient a is the slope of the linear regression, the correlation coefficient R^2 is also indicated. The orange colored part corresponds to the standardization of each instrument according to the PWD, the values of a give the factor of standardization.

	wind	3m/s	5m/s	6 m/s	7 m/s
30°	total	29	74	75	28
	2 to 14 µm	31	58	68	30
	14 to 29 µm	25	94	86	26
60 °	total	71	88	95	93
	2 to 14 µm	65	82	93	87
	14 to 29 µm	80	96	99	99
90°	total	46	95	96	98
	2 to 14 µm	41	93	95	97
	14 to 29 µm	55	97	99	100

Table 4: FSSP concentration loss in percentage compared to the isoaxial measurement concentration, as a function of the wind speed and the angle between wind direction and instrument orientation. For each angles and wind speed values, this percentage is computed for the entire size range (2 to 45µm), the small particles (2 to 14 µm) and the large particles (14 to 29µm).

	wind	3m/s	5m/s	6 m/s	7 m/s
30°	total	15	43	34	21
	2 to 14 µm	16	32	34	21
	14 to 29 µm	18	74	35	31
60 °	total	45	55	68	62
	2 to 14 µm	41	44	67	50
	14 to 29 µm	62	84	71	90
90°	total	37	58	47	54
	2 to 14 µm	33	59	52	52
	14 to 29 µm	49	67	16	52

Table 5: Same as Table 4, for the FM 100

Figures

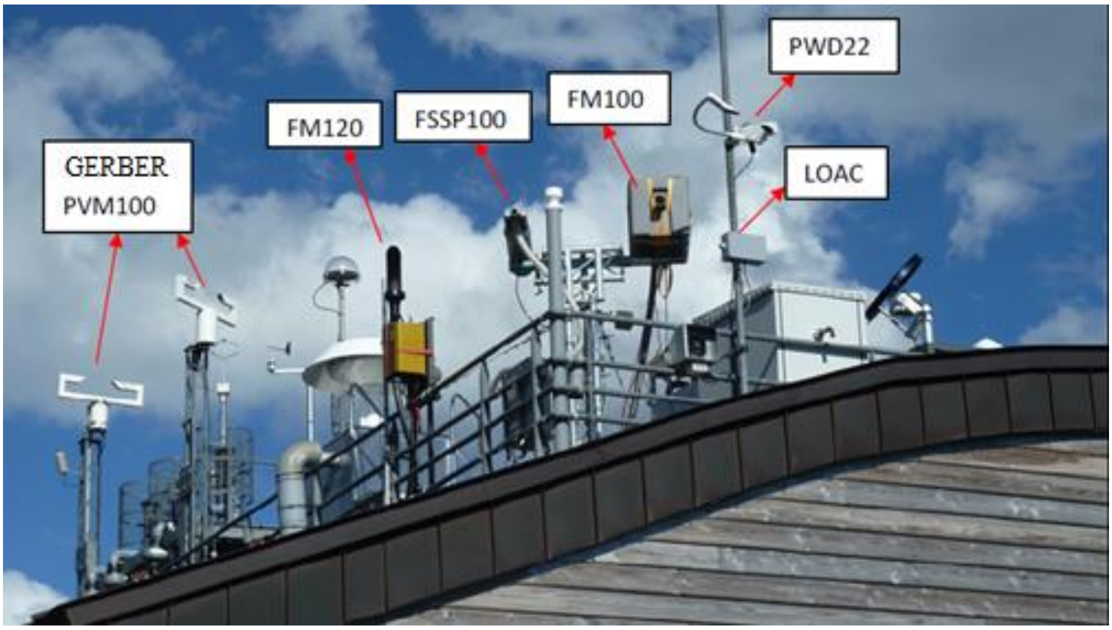

a)

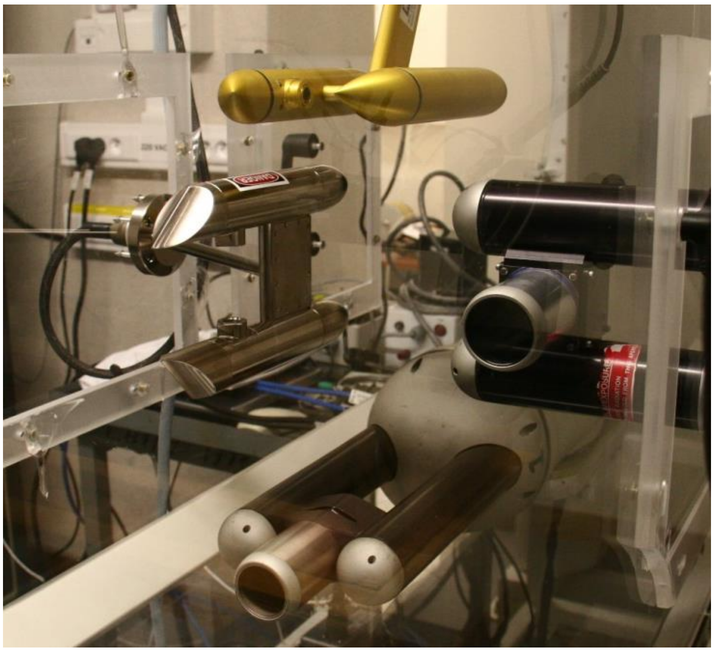

b)

Photo 1: a) Instruments set-up on the roof. The FSSP and the FM 100 were placed on the mast, which can be oriented manually, so the direction where pointed these two instruments can be chosen and b) instruments set-up in the wind tunnel, the SPP at the right, the CDP 1 at the top and the CDP 2 at the left.

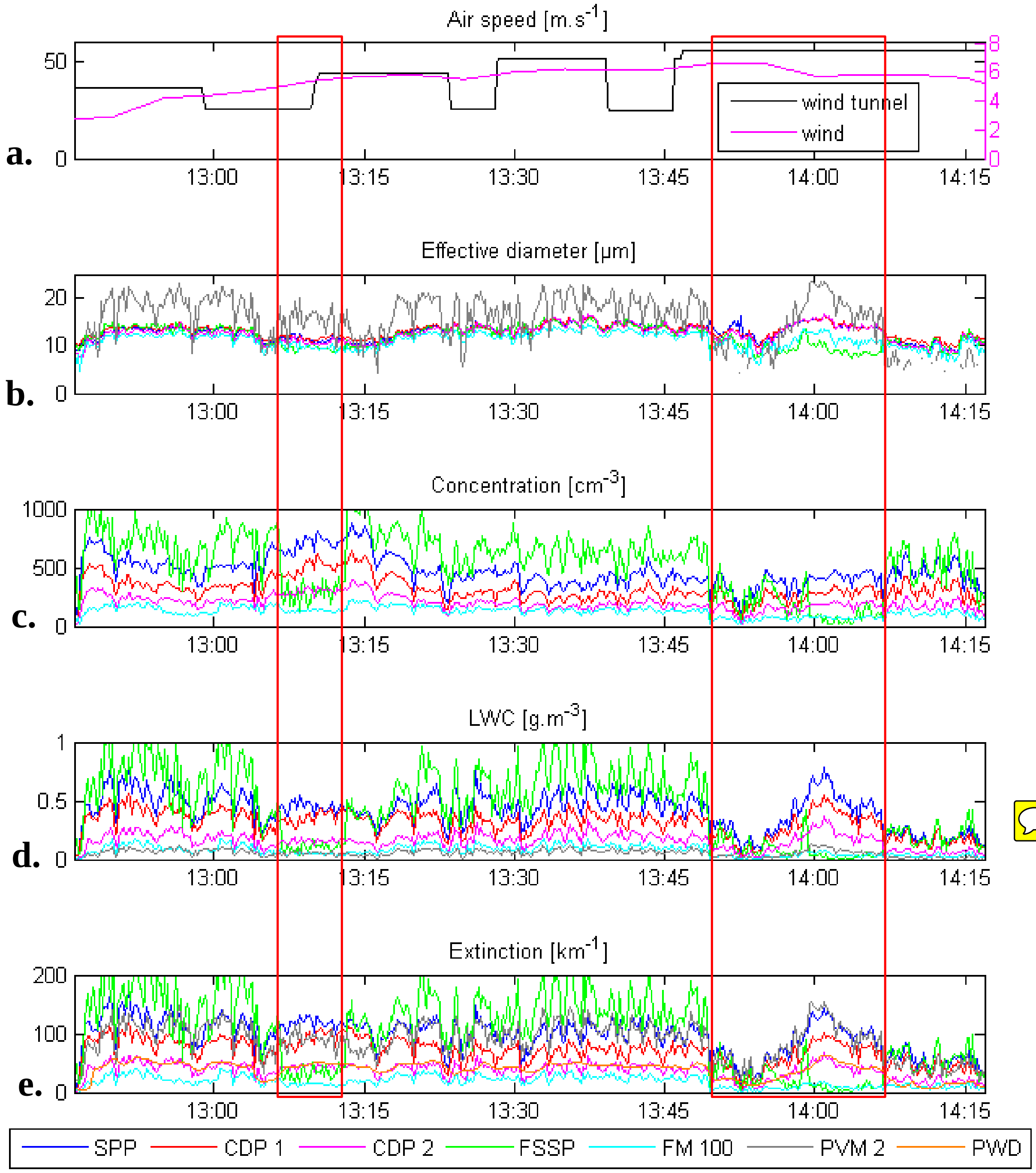

Figure 1: Time series of the 16 May experiment of the main measured parameters: a. ambient wind speed (purple) and wind tunnel air speed (black); b. effective diameter; c. concentration; d. LWC and e. extinction. The data are 10 seconds averaged, except for the PWD measurements performed with a 1 minute time resolution. The red-framed parts of the time series correspond to additional experiments where the orientation of the instruments on the mast was changed (for the FM 100 and the FSSP).

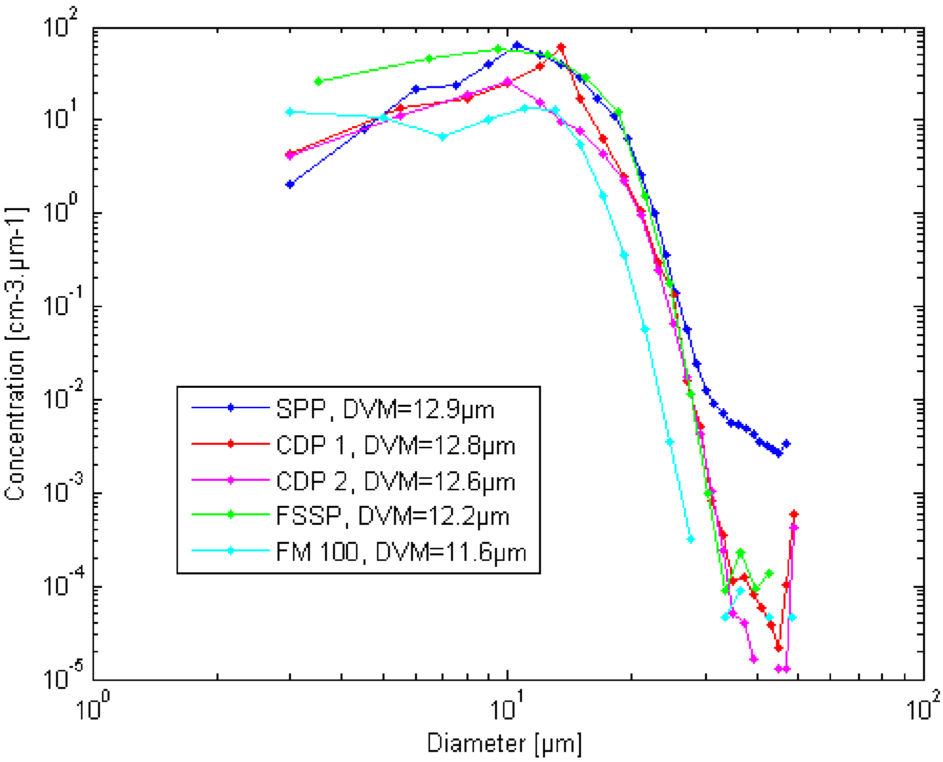

Figure 2: Averaged size distribution for the 16th of May over the period of time shown in figure 1 (i.e. 12:46 PM to 2:17 PM). The color corresponds to the different instruments displayed in the legend. The average median volume diameter DVM is also shown.

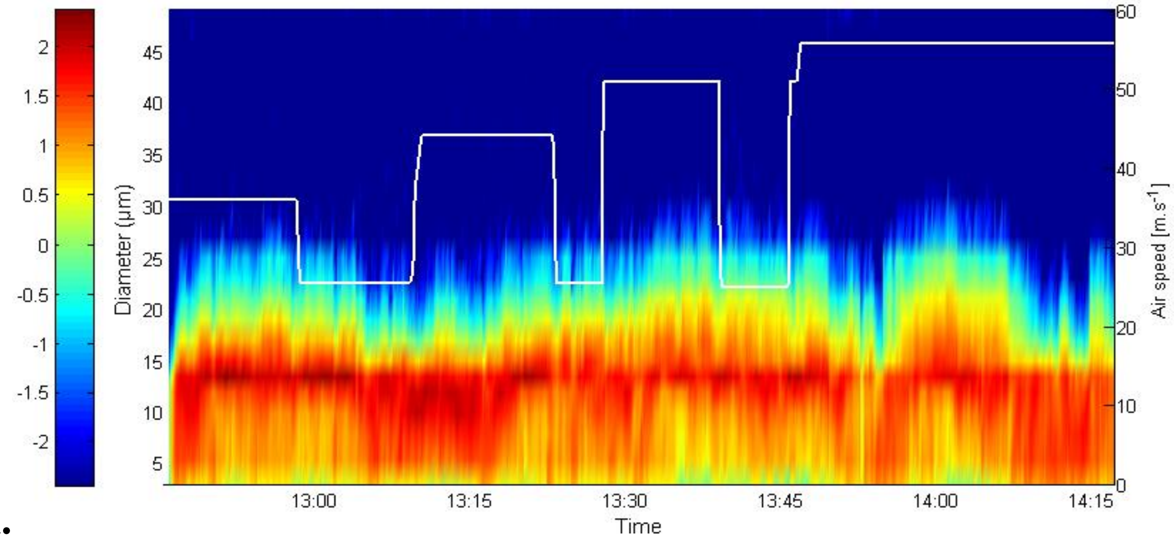

a.

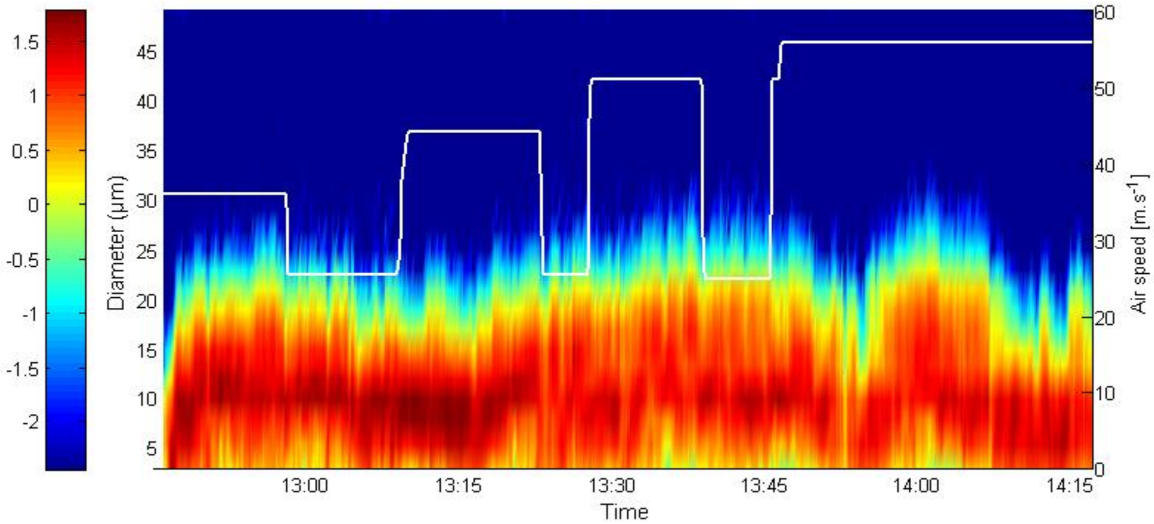

b.

Figure 3: Time series of the 10 seconds average size distributions of CDP1 (a) and CDP2 (b), for the 16th of May. The logarithmic values of the concentration for each size bin of the CDP in $cm^{-3}.\mu m^{-1}$ are color-coded. The air speed applied in the wind tunnel is plotted in white.

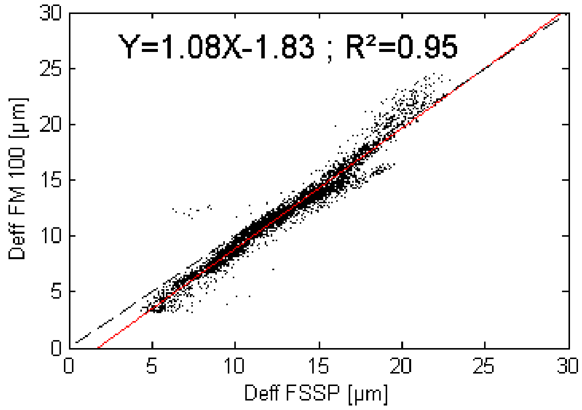

a.

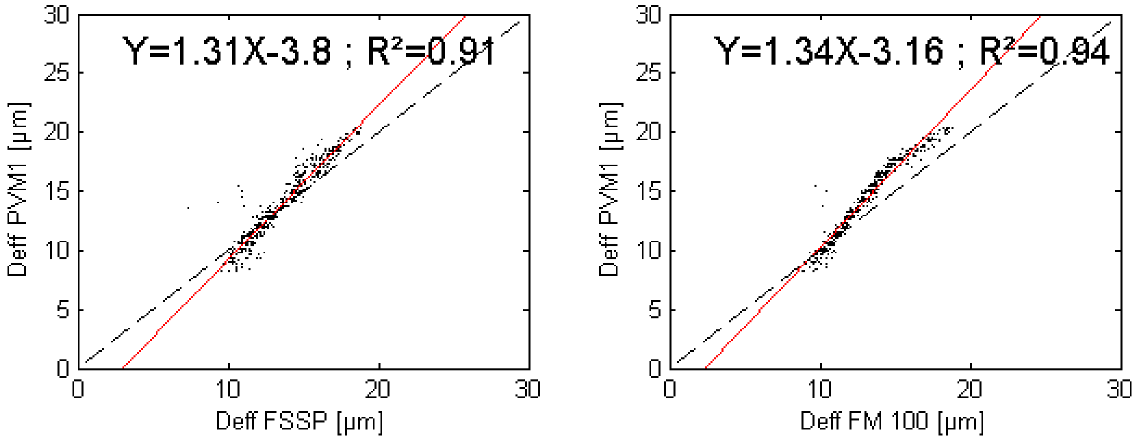

b.

Figure 4: a. Comparison between the 1-minute averaged effective diameters of the FM 100 and the FSSP

b. Comparison between the 5-minute averaged effective diameters between the PVM1 and the FSSP (left) and with the FM 100 (right).

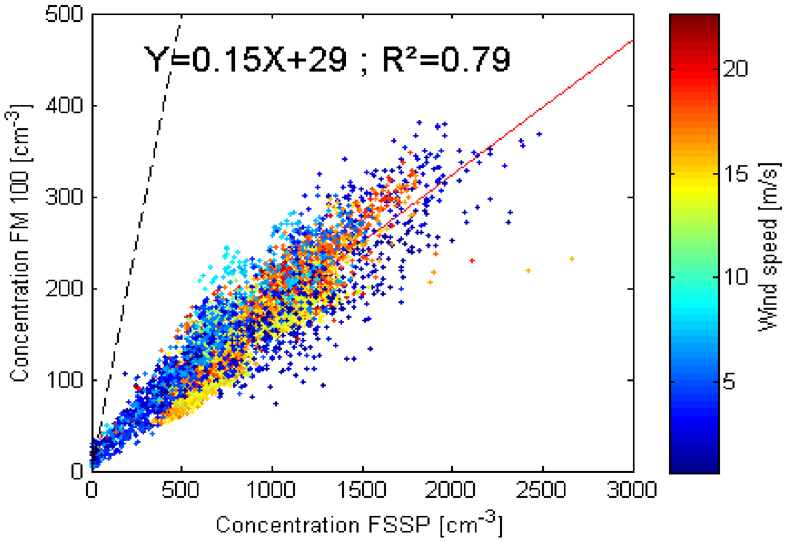

Figure 5: 1-minute averaged concentration in cm^{-3} measurements obtained from the FM 100 as a function of the FSSP concentration of the FSSP. The color shows the values of the wind speed.

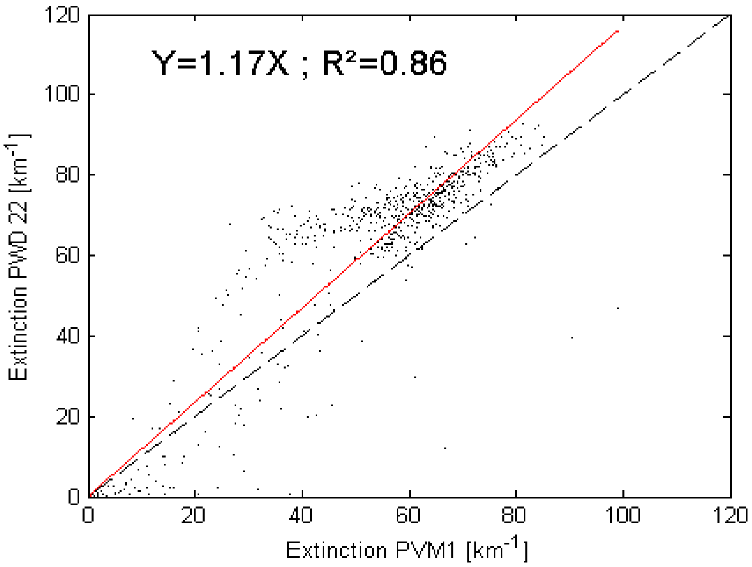

Figure 6: Scatter plot of the PWD and PVM1 5-minute average extinction coefficients.

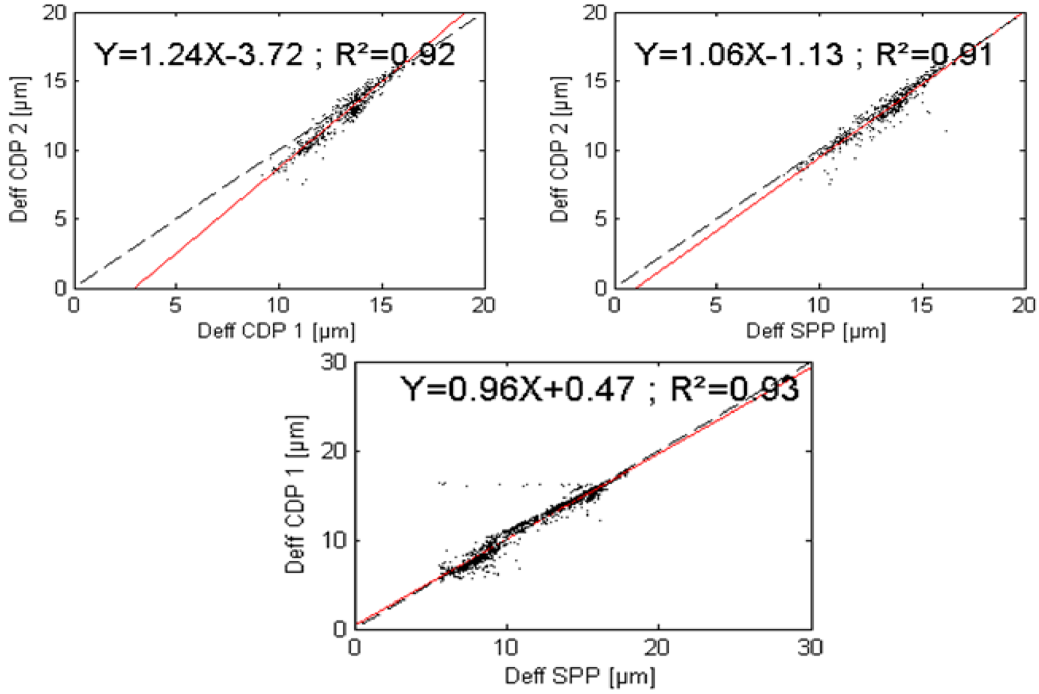

a.

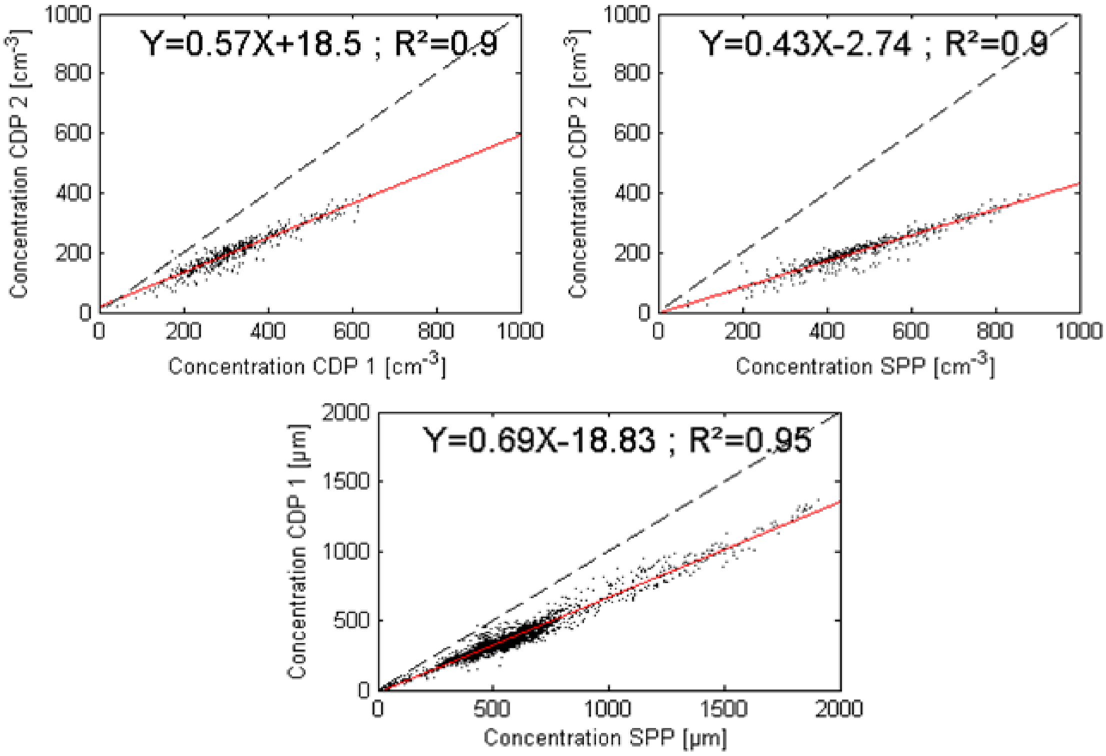

b.

Figure 7: (a) 10 seconds averaged data comparison of the effective diameter measured by the instruments installed in the wind tunnel, i.e. the CDP1, the CDP2 and the SPP; and (b) 10 seconds averaged data comparison of the concentration measured by the instruments installed in the wind tunnel.

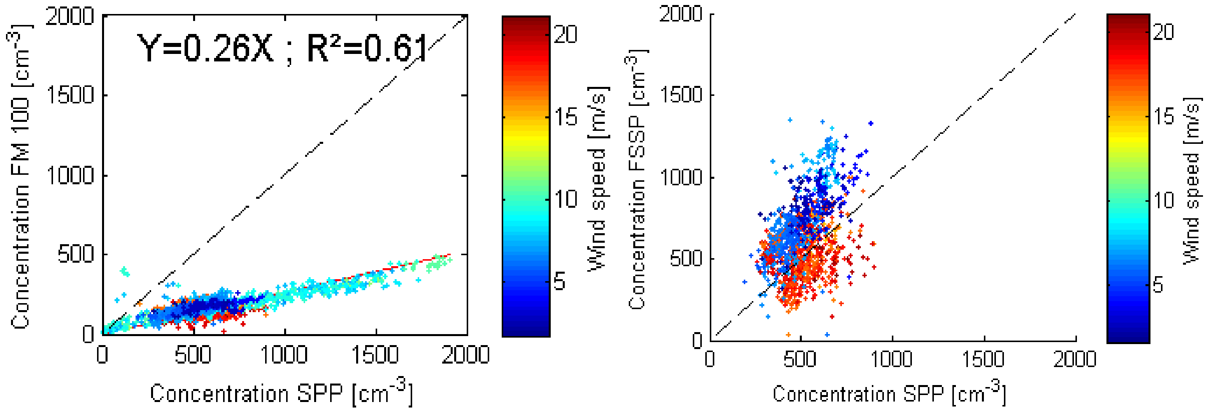

Figure 8: Scatter plots of the 10-second averaged concentrations measured by the FM 100 (left) and the FSSP (right), in ambient conditions, with the wind tunnel SPP. The color reveals the ambient wind speed.

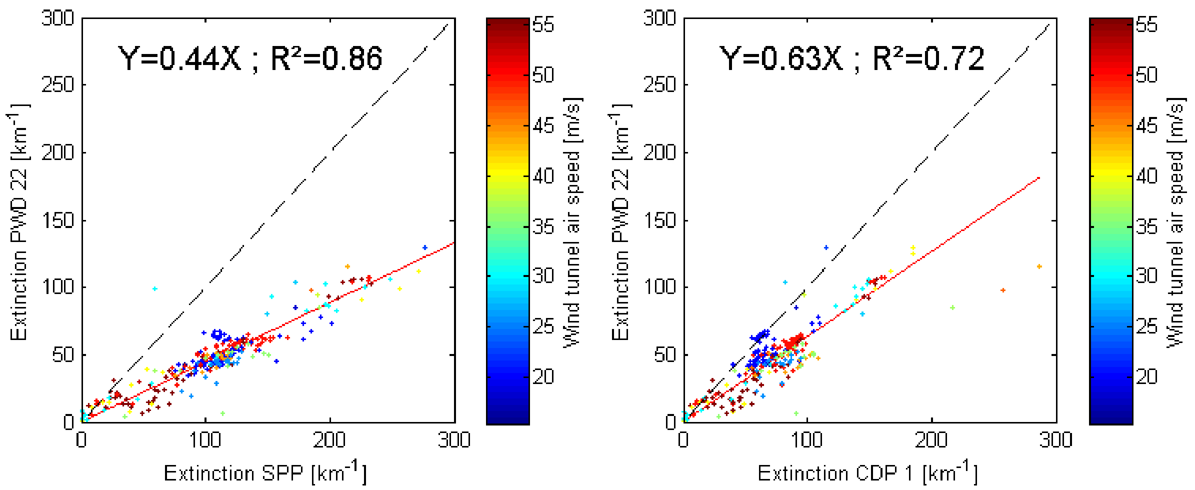

Figure 9: 1 minute averaged SPP and CDP 1 extinctions compared with the PWD extinction for the four wind tunnel experiments. The air speed applied in the wind tunnel is shown on the colorbar.

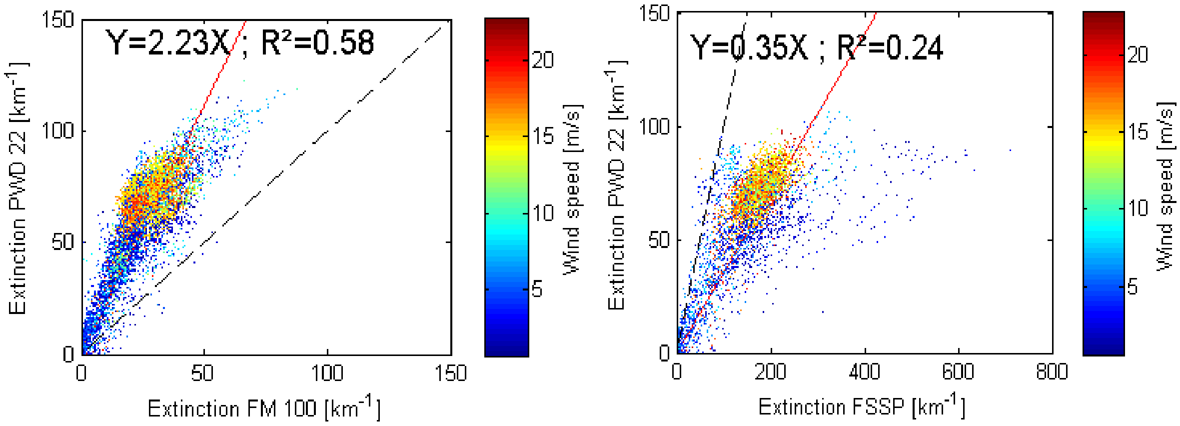

Figure 10: 1 minute averaged FSSP and FM 100 extinctions versus the PWD extinction during the entire ROSEA campaign. The measurements have been selected for cloudy events. The red line reveals the linear correlation and the colorbar shows the values of the wind speed.

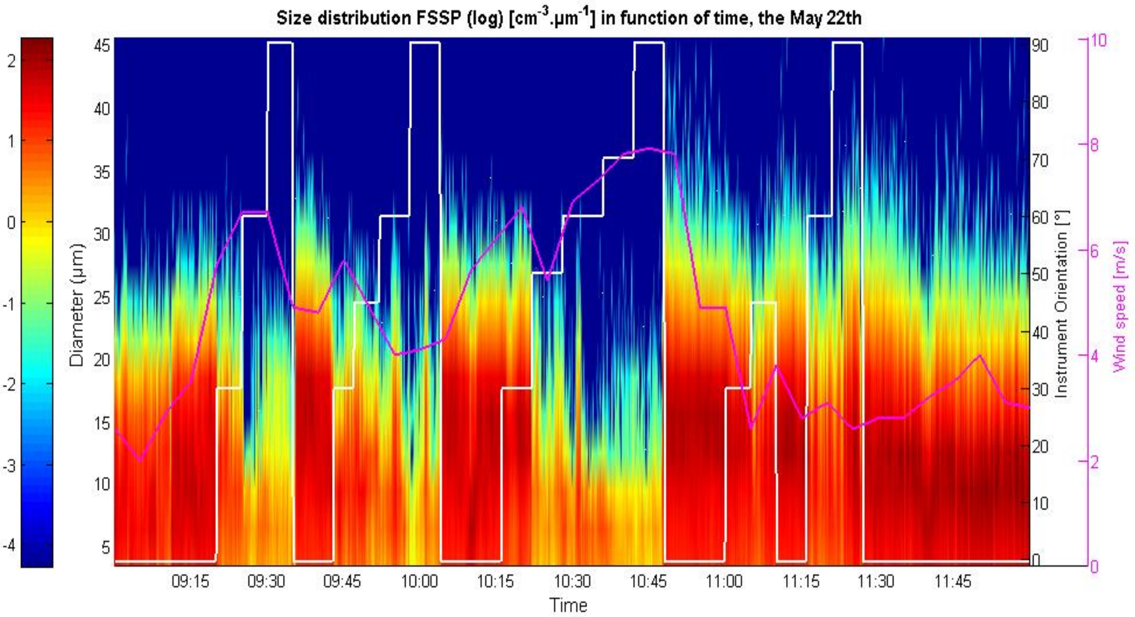

a.

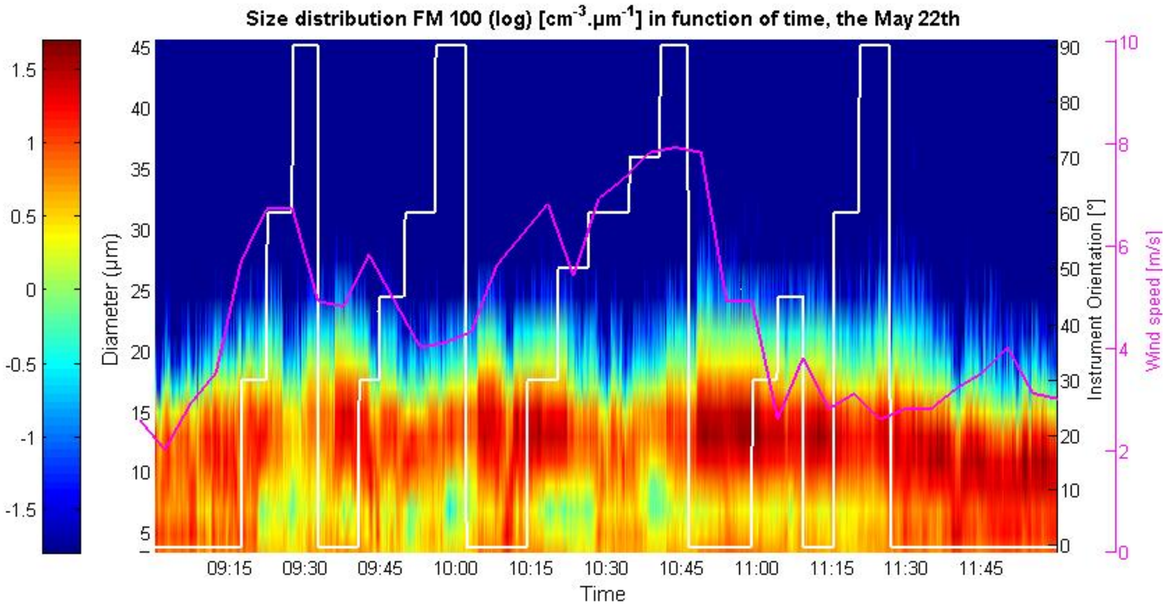

b.

Figure 11: FSSP (a) and FM 100 (b) time series of the size distribution [$cm^{-3}.\mu m^{-1}$] during May the 22nd. The angle between the wind direction and the mast direction is plotted in white and the wind speed in magenta.

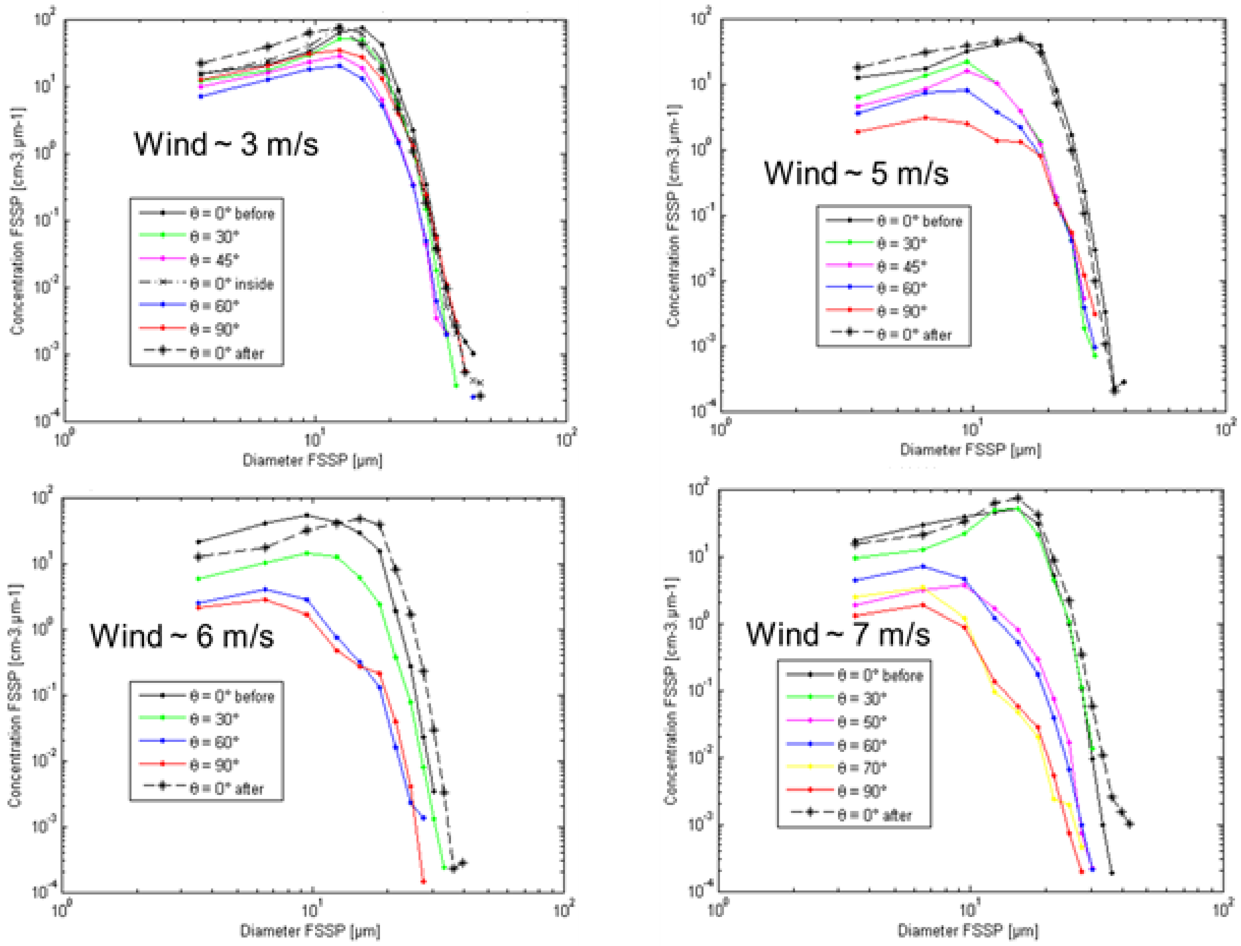

Figure 12: FSSP size distribution averaged for each angle θ corresponding to the angle between the wind direction and the instrument orientation, for the four manipulations. The averaged wind speed is indicated for each experiment.

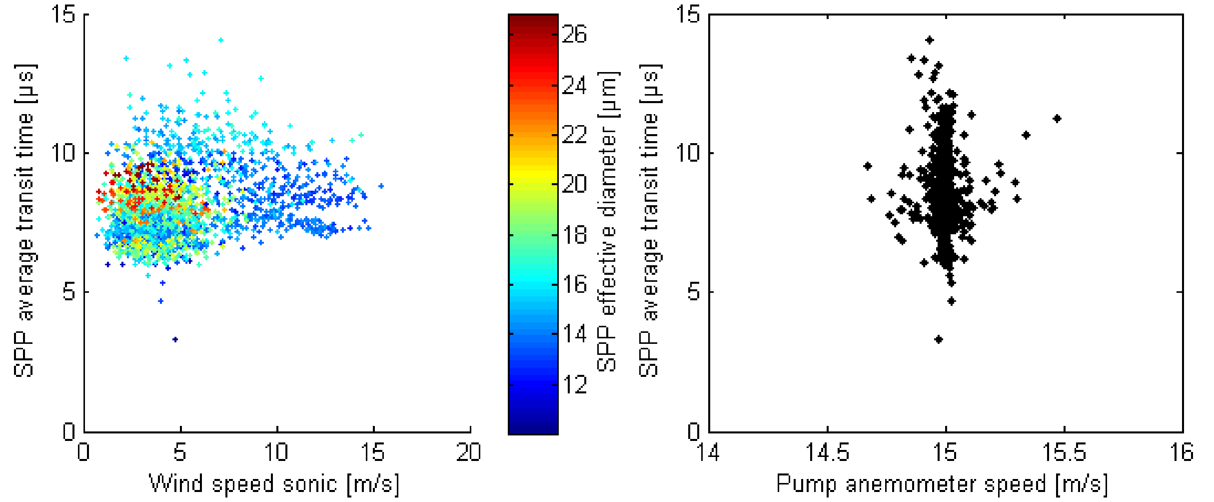

Figure 13: SPP average transit time as a function of the ambient wind speed (left) and of the pump suction speed (right). The color shows the effective diameter measured by the SPP. The data are averaged over 1 minute.

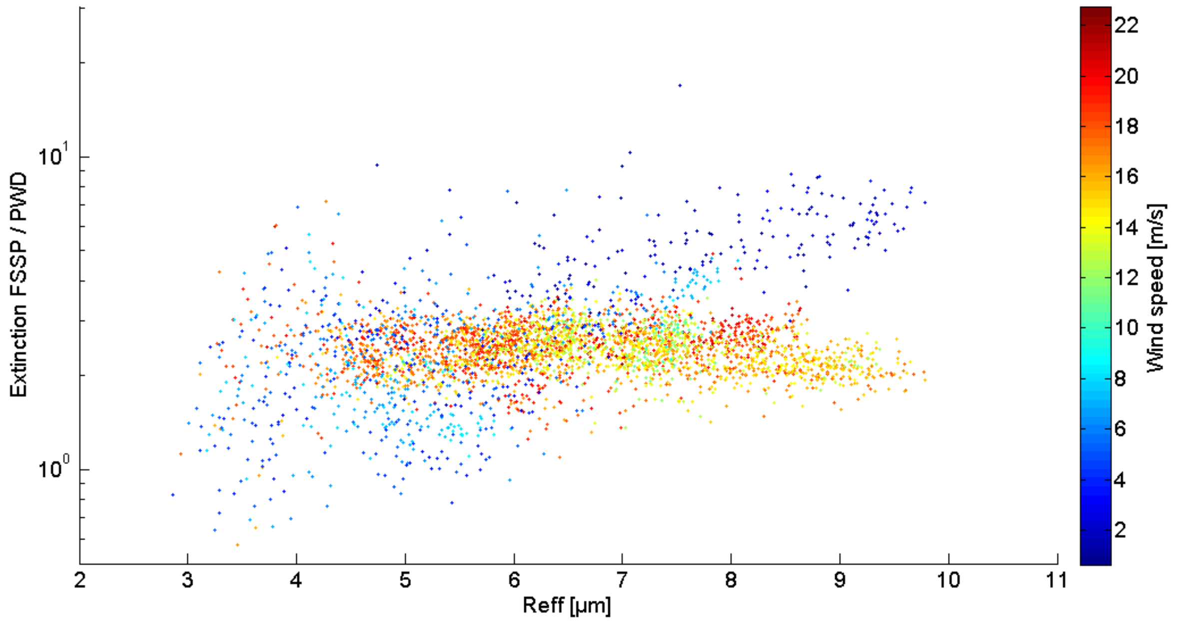

Figure 14: Extinction ratio between the FSSP and the PWD as a function of effective radius of cloud droplets and ambient wind speed, during the ROSEA campaign.